TOP DOWN AND BOTTOM UP:

A COMPARISON OF NANNOFOSSIL SR/CA AND BENTHIC FORAMINIFERAL ACCUMULATION RATES AS PALEOPRODUCTIVITY INDICATORS

by

Amanda J. Waite

A thesis submitted to the Faculty of the University of Delaware in partial fulfillment of the requirements for the degree of Master of Science in Marine Studies

Summer 2005

TOP DOWN AND BOTTOM UP:

A COMPARISON OF NANNOFOSSIL SR/CA AND

BENTHIC FORAMINIFERAL ACCUMULATION RATES

AS PALEOPRODUCTIVITY INDICATORS

by

Amanda J. Waite

Approved: _____

Katharina Billups, Ph.D.
Professor in charge of thesis on behalf of the Advisory Committee

Approved: _____

Nancy Targett, Ph.D.
Interim Dean of the College of Marine Studies

Approved: _____

Conrado M. Gempesaw II, Ph.D.
Vice Provost for Academic and International Programs

ACKNOWLEDGMENTS

First and foremost, I must acknowledge Dr. Cynthia Domack for sparking an interest in geology, oceanography and everything paleo, which continues to grow with each passing day; the passion that she exudes, in everything she does, is both an inspiration and a force to be reckoned with. To Dr. Katharina Billups, I owe many thanks for both the opportunities which she had provided me and her, for lack of a better term, infectious ambition; it has been a quick ride, but one filled with many lessons that I will carry with me into the future. Professional gratitude also goes out to Dr. David Hutchins and Dr. Heather Stoll for being willing participants in my committee and offering their expertise, to Rosalind Rickaby for being so kind as to run all of my samples, to Liselotte Diester-Haass for sharing her data and insight, and to Samantha Gibbs for a crash course in nannos, candid advice and continued collaboration.

On a more personal level, I must praise my parents for continuing to both tolerate and support me no matter what I do. I'd also like to remind them that they should breathe a small sigh of relief as my sample size has jumped from foot long slabs of shale to specs unnoticeable to the naked eye (meaning there may still be some hope for the extensive collection mounting in my old room). Though my lab mates Carolyn and Kate have since left me to my own devices, they continue to offer invaluable advice and friendship and the CMS 'family' as a whole has made my time in Delaware both enjoyable and unforgettable, for which I am extremely grateful. To my friends outside of CMS, and especially Nick, thank you for assisting, listening, smiling, nodding, supporting and (in more ways than one) coming along for the ride...

TABLE OF CONTENTS

LIST OF TABLES

LIST OF FIGURES

ABSTRACT

This study compares productivity records from two different proxies, nannofossil Sr/Ca as an indicator of surface ocean primary productivity and benthic foraminiferal accumulation rates (BFAR) as an indicator of consumption at the seafloor, using late Miocene-early Pliocene sediments from Ocean Drilling Program (ODP) cores at Atlantic Ocean Sites 982 and 925. The research provides the unique opportunity to relate multiple aspects, both physical and geochemical in nature, from a single set of synchronous samples in order to reconstruct paleoproductivity. Despite a number of uncertainties uniquely related to each proxy, the productivity reconstructions share numerous similarities. Records from both sites show a marked increase in productivity in the long term trend during the study interval, including increasing values of BFAR [Diester-Haas *et al.*, in press] and bulk (0.8 to 20.0 μm) nannofossil Sr/Ca at ~5 Ma at Site 982, and an increase in measured BFAR [Diester-Haas *et al.*, in press] and fine fraction (0.8 to 8.0 μm) Sr/Ca that are synchronous at ~6 Ma at Site 925. Additionally, the records share a number of similarities in small scale maxima and minima. This suggests that a link is preserved in the geologic record between surface ocean productivity, export production and the reflection of them on the seafloor. Furthermore, the results of this study support evidence for an ocean wide increase in productivity during the late Miocene-early Pliocene study interval.

Species effects on the Sr/Ca record are examined here using a high resolution nannofossil species abundance record published by Gibbs *et al.* [2004] for ODP Site 926. Results of this analysis show cyclic insolation-like fluctuations in measurements of the coarse fraction (8.0 to 20.0 μm) nannofossil Sr/Ca only. These patterns are consistent with orbital forcing and parallel fluctuations in *Discoaster* and *Florisphaera profunda* abundances. This suggests that coarse fraction Sr/Ca may be dominated by a record of discoaster productivity, as total *Discoaster* abundances are at their minima in association with high magnetic susceptibility and low insolation. Furthermore, this suggests that *Discoaster* abundances (and potentially calcification and/or growth) may be controlled by environmental conditions (nutrient levels and/or temperature) varying on orbital time scales. This may be associated with, at least in part, orbitally driven terrigenous supply (including clays, organic matter and nutrients) to the Ceara Rise from the Amazon River or insolation guided changes in the upper ocean hydrography (photic zone and/or thermocline depth).

Overall, this study documents remarkably good agreement between the BFAR and nannofossil Sr/Ca proxies for productivity, as well as good support for an increase in Atlantic Ocean productivity during the late Miocene-early Pliocene interval. The presence of some inconsistencies between the proxy records (e.g. differing trends between fine and coarse fraction Sr/Ca at Site 925 and Site 926 as well as excursions in Site 982 nannofossil Sr/Ca) highlight some of the difficulties faced when interpreting such reconstructions. From here, it might be helpful to utilize improved size fractionation methods and complete down-core assemblage analysis to better constrain species effects on the Sr/Ca records. Also, the construction of synchronous coccolith alkenone records could contribute to the geochemical data presented here by revealing any temperature effects that may be present in

the nannofossil Sr/Ca data. Both the extension of the Site 926 record through the Miocene-Pliocene interval and heightened resolution at Site 925 may also enhance interpretations. Ultimately, this research emphasizes the complex nature of paleoproductivity reconstructions and their interpretation and provides a strong argument for the coupling of numerous paleoproductivity proxies in paleoceanographic studies.

Chapter 1

EXPLORING THE LINK BETWEEN PRODUCTIVITY PROXIES

1.1 Introduction

The geologic record preserved within marine sediments affords the unique opportunity to compare multiple proxies and paleo indicators within one set of samples. Over the past few decades paleoceanography and paleoclimatology have undergone an empirical evolution, as proxies have shifted from a physical approach to one more geochemical in nature. Proxies for paleoproductivity are no exception and this project aims to explore this development, as well as the extensive natural archives found in the deep sea, in order to determine whether or not a link is evident between the surface ocean production of organic matter through nannofossil Sr/Ca ratios and deep ocean consumption as captured in benthic foraminiferal accumulation rates (BFAR).

What occurs in the temporal and spatial expanse between the surface and deep ocean remains ambiguous. Primary productivity within the surface oceans not only plays a significant role in the carbon cycle and transfer of carbon from the surface to the deep, but can also be a reflection of hydrographic and environmental conditions at any given time. A better understanding of these two proxies and their relationship to each other should contribute to a more complete comprehension of the oceans' CO_2 sources and sinks, better modeling for atmospheric changes over glacial and interglacial time scales [Stoll and Schrag,

2000], and a clarified perspective on carbon transport and climate change in the modern world.

The research project detailed here began as a comparison of pale proxies for productivity; the intent being to generate a record of Miocene-Pliocene primary productivity for two hydrographically different Atlantic Ocean locales (Figure 1.1) using nannofossil Sr/Ca ratios, and to compare this record to recently compiled BFAR measurements for synchronous intervals at the same sites [Diester-Haass *et al.*, in press]. The published BFAR data shows a marked increase in productivity in the Atlantic Ocean during this time interval, suggesting that there is a signal in the sediments that can be sought in the surface proxy reconstructions.

In 2004, Gibbs *et al.* published a paper quantifying Pliocene nannofossil assemblage changes at a site that is a close neighbor to one of the Atlantic sites studied here. This affords the unique opportunity to measure high resolution nannofossil Sr/Ca ratios on the same intervals for which species counts are already complete. While the time interval at this third site is not the same as the others used in the project, the resolution is high and allows for an investigation of paleoproductivity on orbital time scales (those related to the eccentricity, obliquity and precession of the Earth's orbit).

With the development and utilization of any paleoceanographic proxy comes a series of uncertainties and limitations to be considered. While proxies like BFAR provide a number of advantages as indicators of productivity, they are heavily reliant upon sedimentation rates, and through this limit both the application and interpretation of the records which they generate. On the other hand, nannofossil Sr/Ca appears to hold the potential to create exclusively geochemical records of paleoproductivity which are

unconstrained by sedimentation rates offering an advantage over some of its counterparts. Overall, the generated geochemical records for paleoproductivity, when coupled with other proxies, elucidate the complexities faced in the development, application and interpretation of paleoceanographic proxies as well as the benefits to be gained from collaboration between various spheres, from micropaleontology and biology to geochemistry.

This project was funded by a grant from the Petroleum Research Fund of the American Chemical Society awarded to Dr. K. Billups and personally obtained grants in aid of research from the Geological Society of America and Sigma Xi.

1.2 Background

1.2.1 Marine primary productivity

Primary productivity, or the amount of plant tissue formed by photosynthesis over time, can play an instrumental role in oceanographic research and the study of modern and ancient climates. This is most pronounced in terms of primary productivity in surface waters and its association with the transfer of carbon between the atmospheric and oceanic reservoirs. While the factors effecting marine primary productivity (like light availability, nutrients and hydrography) are fairly well understood, those that control the amount of organic matter transported to the seafloor and preserved within the geologic record are less well documented. Export production of carbon from the photic zone of cooler regions with higher seasonal variability may be greater than that from warmer oligotrophic regions due to faster microbial decomposition at higher temperatures. In addition, studies have shown that export production is not exclusively controlled by surface ocean productivity [Lampitt and Antia, 1997].

The factors controlling how much organic carbon produced at the ocean's surface ultimately makes it to the seafloor are quite diverse. Boyd and Newton [1999] argue that phytoplankton community structure can be a dominant control on particulate organic carbon (POC) flux. Their study shows that the sinking of large cells may have a disproportionate effect on organic carbon flux and ultimately the regulation of the biologic pump [Boyd and Newton, 1999]. On the other hand, Yamanaka and Tajika [1996] highlight the importance of both the amount of POC produced and the vertical distance it must travel on the efficiency of transfer, where the distance is considered in terms of the depth at which biogenic particles will be remineralized. Francois *et al.* [2002], take this a step further and state that the efficiency of organic carbon transfer shares a direct relationship with carbonate flux and an indirect relationship with water depth and seasonality; describing the 'ballasting' effect of carbonate and the subsequently heightened transfer efficiency of the carbonate producers. Through this function, organic carbon formed in primarily carbonate producing regions would be transported to greater depths before being remineralized than that in regions dominated by opal production [Francois *et al.*, 2002]. Francois *et al.* [2002] suggest that even though less organic carbon is produced in warmer more oligotrophic carbonate producing regions, a greater portion of it is able to make it to the sediment-water interface via the ballasting effect than that in nutrient enriched biogenic silica producing areas.

In the discussion of primary productivity and global carbon/carbonate cycles, it is vitally important to consider the part which coccolithophorids play as primary producers. Coccolithophorid phytoplankton live within the photic zone and have an extensive distribution throughout the Earth's oceans, though they do not generally extend further north than 70º latitude [Bown, 1998]. For the most part, coccolithophorids thrive in warm,

oligotrophic, mid-ocean regions, however, both individual species and the population as a whole show distinct ecological tolerance. Distribution patterns appear to be tied to temperature conditions as well as nutrient (e.g. nitrate and phosphate), trace element and vitamin (e.g. iron and zinc) availability associated with oceanic circulation [e.g. Bown, 1998], hydrographic regimes, vertical stratification of the assemblage and seasonal mixing [e.g. Ziveri *et al.*, 1995; Bown, 1998; Cortés *et al.*, 2001; Haidar and Thierstein, 2001].

Coccolithophorid phytoplankton secrete calcium carbonate ($CaCO_3$) plates known as coccoliths and, in doing this, are considered one of the greatest producers of calcite on Earth [e.g. Westbroek *et al.*, 1994; Rost and Riebesell, 2004]. Both global in occurrence and capable of producing large blooms, coccolithophorid productivity, the calcite it forms and its export from surface waters has repercussions on carbon flux within the oceans [Westbroek *et al.*, 1993; Winter and Siesser, 1994; Rost and Riebesell, 2004]. Because of this, coccoliths may hold the key to a better understanding of these cycles, including information on past variations in the rain ratio between inorganic and organic carbon and an improved estimation of the CO_2 resulting from carbon isotope fractionation in coccolithophorids [Stoll and Schrag, 2000; Stoll *et al.*, 2002c]. Additionally, coccolith minor element analysis can be used in accord with carbon isotope fractionation in alkenones to estimate dissolved pCO_2 levels in surface oceans of the past [e.g. Stoll *et al.*, 2002a; Stoll *et al.*, 2002b]. In this regard, coccolithophorids provide a top down view of carbon transfer from the atmosphere to the ocean and ultimately the seafloor, however, the processes by which this occurs are complex and not well understood even in the modern ocean.

1.2.2 Top down: Nannofossil Sr/Ca ratios

While an extensive amount of research has been performed on minor and trace element fluctuations within ocean carbonates in an effort to better understand past climates and the oceans' systems, the vast majority of this has focused on foraminiferal and coral sources of carbonate. This comes despite the fact that, in some areas, nearly 80% of the carbonate in the sediments is in the form of coccolith calcium carbonate [Stoll and Schrag, 2000]. Given the significant role that coccolithophorids hold as the only primary producers which are widely distributed *and* preserved within the fossil record, geochemical analysis of nannofossils (like coccoliths) could play a valuable part in paleoceanographic research studies.

It is known that as $CaCO_3$ precipitates in the world's oceans, strontium can be exchanged for calcium within the crystalline lattice. This occurs because Sr and Ca share similar sizes and identical charges (+2). The Sr/Ca of a coccolith is directly related to the Sr/Ca of seawater; Sr/Ca in calcite has been shown to vary with the rate of calcite production, and ultimately, growth rate. This is to say that at low rates of particle growth, equilibrium is approached between the surface water and the carbonate, resulting in minimal fractionation and a low degree of Sr substitution for Ca in the coccolith, producing low Sr/Ca levels; if, however, conditions are such that particle growth rate is high, then equilibrium cannot be maintained between the surface oceans and the solid; this results in a high degree of substitution of Sr for Ca and high observed Sr/Ca values (Figure 1.2) [e.g. abiogenic- Lorens, 1981; Watson, 1996, Watson, 2004; biogenic- Stoll and Schrag, 2000; Stoll and Ziveri, 2004].

Research has shown coccoliths to demonstrate much more pronounced fluctuations in Sr/Ca than foraminifera, suggesting that a good percentage (nearly 15%) of the variation observed in coccolith Sr/Ca must result from changes in Sr partitioning within the coccolith carbonate, rather than just fluctuations in seawater Sr/Ca (which varied by less than 2%) [Stoll and Schrag, 2000]. This has led to a search for other factors influencing Sr partitioning in coccoliths. Stoll and Schrag's [2000] study finds coccolith Sr/Ca to covary with $CaCO_3$ rain rate in deep sediment traps, possibly indicating a correlation between coccolith Sr/Ca and the growth and calcification rates of coccolithophorids. In 2002, Rickaby *et al.* confirm the connection between coccolith Sr/Ca, growth rate and calcification and further suggest that the incorporation of Sr into the coccolith is controlled by a rate dependent selection of the cell. This selection would prevent the biological pumping of the larger Sr ions into the intracellular vesicle of the coccolithophorid which produces the coccolith, and thereby influences the composition of the coccolith itself.

A clear relationship between coccolith Sr/Ca and average productivity has been demonstrated by the field studies of Stoll and Schrag [2000]. From this the authors conclude that coccolith Sr/Ca covaries with primary productivity near the equator [Stoll and Schrag, 2000]. Additionally, an examination of coccolith dominated Cretaceous carbonates [Stoll and Schrag, 2001] shows good temporal matching between nannoplankton ecology, surface nutrient fluctuation, nannoplankton productivity records and Sr/Ca variations suggesting that there are productivity related factors affecting Sr partitioning in carbonate nannoplankton and that a record of this is preserved within the geologic record. A synthesis of Sr/Ca work from Stoll and Ziveri [2004] ultimately suggests that there is a correlation between coccolith Sr/Ca and coccolithophorid productivity, and that this productivity would

most likely be driven by nutrient and/or C limitation rather than that of light [e.g. Stoll *et al.*, 2002c]. In a compilation of Cenozoic records [Billups *et al.*, 2004] the authors note a sizeable increase in bulk carbonate Sr/Ca that can be tied to evidence for a relative rise in oceanic nutrient levels. From this they conclude that Sr/Ca observations reflect, to a certain extent, the effect of nutrient levels on Sr partitioning on longer geologic time scales [Billups *et al.*, 2004]. Billups *et al.* [2004] further hypothesize that the Sr/Ca ratios of bulk pelagic carbonates are varying in accord with productivity at the sea surface, but are careful to note the limitations associated with the interpretation of these results.

The results of a laboratory study by Stoll *et al.* [2002a] show Sr partitioning within coccolithophorids to be equally correlated with both calcification rate and temperature. The work found that, at constant temperature, Sr partitioning within a number of species has a linear relationship to calcification rates consistent with kinetic effects on Sr partitioning in abiogenic calcites [Stoll *et al.*, 2002a]. This is further emphasized by Stoll *et al.* [2002b] who, from continuous cultures of *Emiliania huxleyi*, were able to conclude that coccolith Sr/Ca ratios are much more sensitive to changes in temperature than to variation in calcification growth rate resulting from light limitation. While this contrasts with the earlier findings of Stoll and Schrag [2000] that show coccolith Sr/Ca and growth rate maxima in correlation with temperature minima, the discrepancy between field and culture data is a reoccurring theme in coccolith studies and most likely results from the inability of laboratory settings to mimic natural environments as well as the lack of nutrient limitation in some culture studies. A review by Stoll *et al.* [2002c] highlights the fact that laboratory cultures appear to demonstrate a much more noteworthy temperature effect than field studies would predict.

The synthesis of Sr/Ca work, from Stoll *et al.* [2002c], offers a series of chemical and biological factors which may ultimately control Sr/Ca, both directly and indirectly tied to productivity. They suggest that controls may be related to kinetic or thermodynamic effects within the formation of the crystalline lattice, an enrichment of Sr on the growing crystal's surface or the biological control of intracellular fluid proposed by Rickaby *et al.* [2002]. Studies like that of Billups e*t al.* [2004], however, seem to offer evidence for a biogeochemical control on Sr uptake in biogenic calcite.

In addition to the published BFARs, the nannofossil Sr/Ca records will also be compared to the accumulation of carbonate ($CaCO_3$) in the sediments, which has been measured at the sites in previous studies [Curry *et al.*, 1995; Jansen *et al.*, 1996]. Carbonate accumulation rates are often used to infer surface water productivity if it can be assumed that dissolution in the deep ocean is negligible [e.g. Peterson *et al.*, 1993; Farrell *et al.*, 1995; Murray and Peterson, 1997; Grant and Dickens, 2002; Diester-Haass *et al.*, in press]. Intuitively, increased nannofossil productivity should result in an increased rate of carbonate accumulation at the seafloor, however, accumulation rates are limited by age control as well as dissolution. Hence, this study should yield some insight into how consistent published accumulation rates are with carbonate production proxies unaffected by age model uncertainties.

1.2.3 Bottom up: Benthic foraminiferal accumulation rates

Benthic foraminifera at the seafloor rely heavily upon organic matter transported from the photic zone for sustenance. Because of this, the quantity and quality of the export production from surface waters can be reflected in benthic faunal abundance. Studies from

across the globe have shown benthic foraminiferal species richness to increase with increasing organic carbon flux to the seafloor [e.g. Herguera and Berger, 1991; Nees, 1997; Schmiedl and Mackensen, 1997; Yasuda, 1997; Van der Zwaan *et al.*, 1999; Herguera, 2000]. This provides the foundation for benthic foraminiferal accumulation rates (BFAR) as a proxy for paleoproductivity which has been widely utilized [e.g. Herguera and Berger, 1991; Nees, 1997; Schmiedl and Mackensen, 1997; Van der Zwaan *et al.*, 1999; Diester-Haass *et al.*, 2004; Diester-Haass and Nees, 2004; Diester-Haass *et al.*, in press].

Herguera [2000] presents data collected from core top sediments of the equatorial Atlantic and Pacific Oceans and discusses the response of export production to the seafloor as determined by location, both absolute and hydrographic. Along with this discussion however, comes a calibration for BFAR and organic carbon flux to the seafloor based on relationships between sea surface primary productivity and flux previously described by Berger and Wefer [1990]. Herguera [2000] uses this relationship to develop a simple equation relating paleo primary productivity to BFAR ($pPP = 0.4 * Z * BFAR^{0.5}$; where pPP is the paleo primary productivity reflecting organic carbon flux to the seafloor, Z is the water depth, and BFAR are the benthic foraminiferal accumulation rates as recorded in counts/cm^2/kyr; and BFAR are obtained by multiplying test counts per gram of sediment by the mass accumulation rate). Herguera [2000] cautions that this relationship is based on the assumptions that a) there is a constant relationship between the production of organic matter in the surface ocean and export production, b) the relationship between export production and the amount of organic carbon reaching the seafloor is constant, and c) the export of organic carbon to the seafloor is inversely related to water depth, an idea that holds true as a first order approximation for the open ocean.

While BFAR are the more commonly used productivity proxy of those presented in detail here, they are not without their own challenges and limitations. BFAR are dependent upon sedimentation rates, which are a function of the age model utilized. While some age models have high temporal resolution, others rely on the interpolation of data between widely spaced control points. These control points may span up to tens of thousands of years or even longer when based on biostratigraphy. In these instances, the sedimentation rates are assumed to be constant between the controls, meaning that the resolution of the rates is known on a very coarse scale and any imprecision within it will be reflected within the BFAR data.

1.2.4 The Miocene-Pliocene biogenic bloom

The late Miocene–early Pliocene time period selected for this research is significant to the project design itself. This time interval, just prior to the extensive glaciation of the Northern Hemisphere, is marked by relative warmth around the globe. Evaluation of sediment cores clearly illustrates a period of high productivity and low dissolved O_2 in intermediate waters of the Indo-Pacific region between 3.5 and 9 Ma [Dickens and Owen, 1999], as well as a dramatic increase in biological productivity and carbon burial rates in major upwelling regions [Summerhayes *et al.*, 1995; Diester-Haass *et al.*, 2004]. Increased productivity is also found in the equatorial Indian and Pacific Oceans and the Southern Atlantic [e.g. Peterson *et al.*, 1992; Berger *et al.*, 1993; Farrell *et al.*, 1995; Lyle *et al.*, 1995; Diester-Haass *et al.*, in press]. Furthermore, evidence for this bloom has also been found in low productivity areas of the Indian and Atlantic Oceans [Hermoyian and Owen, 2001; Diester-Haass *et al.*, in press]. In the northwest Pacific Ocean, opal accumulation rates

increase during this period [Rea *et al.*, 1995] and Delaney and Filippelli [1994] found increases in phosphorous accumulation rates to be present on a global scale. This characteristic sediment change has become known as the late Miocene–early Pliocene 'biogenic bloom' interval.

Some researchers have speculated that a large increase in the nutrients available in the ocean, resulting from the Himalayan Plateau uplift and an associated increase in weathering, might be the cause of the bloom [Dickens and Owen, 1999]. Other theories surmise that enhanced deep water flow could transfer nutrients from other regions and lead to increased productivity along divergence zones, as this correlation is clearly represented in the data [Dickens and Owen, 1999]. Regardless of the causes of this bloom, or even its absolute extent, the importance of the interval in the context of this project lies in the fact that a means exists by which productivity, as reflected by both the BFAR and nannofossil Sr/Ca measures, may be altered.

Chapter 2

INVESTIGATIVE APPROACH

2.1 Site selection and regional hydrography

The two Ocean Drilling Program sites chosen for this paleoproductivity investigation, ODP Site 982 and 925, were originally selected by Diester-Haass *et al.* [in press] for their benthic foraminiferal accumulation rate (BFAR) analyses. The initial site selection was based on high carbonate content throughout the study interval, as well as their location in regions which were not likely affected by coastal or open ocean upwelling during the Miocene-Pliocene. These characteristics coupled with the complete BFARs [Diester-Haass *et al.*, in press] and available synchronous sediments for geochemical analysis make them a prime target for this type of proxy comparison. Also, as the results of the benthic foraminiferal counts by Diester-Haass *et al.* [in press] indicate that a noteworthy increase in paleoproductivity exists at both ODP Site 982 and Site 925 (at ~5 Ma and ~6.5 Ma, respectively), a signal should be apparent in the nannofossil Sr/Ca.

2.1.1 Ocean Drilling Program Site 982

The first of the ODP sites chosen for analysis is Site 982 in the North Atlantic and it ultimately acted as a test site for the proposed methods. As an exploratory initial investigation, the main objectives were to determine whether or not nannofossil Sr/Ca ratios

could be generated within an acceptable expected range as well as examining any possible similarities between these records for paleoproductivity and those provided by BFAR as generated by Diester-Haass *et al.* [in press] and $CaCO_3$ from Shipboard Reports [Jansen *et al.*, 1996; Curry *et al.*, 1995].

The sedimentary sequence at Site 982 was drilled within the Hatton-Rockall Basin of the Rockall Plateau along the Arctic Gateway in the Northern Atlantic Ocean (Figure 1.1). At present, it lies at a water depth of approximately 1134 m though it is estimated that the water depth during the middle to late Miocene would have been 100 to 150 m shallower than it is today [Andersson and Jansen, 2003]. Modern upper ocean hydrography at Site 982 is marked by seasonal changes in the depth of the thermocline. These seasonal fluctuations result in a well mixed surface layer during the winter months which brings nutrient-rich waters to the photic zone (Figure 2.1 A) [Levitus and Boyer, 1994].

The high latitude location of Site 982 also lends itself to substantial seasonal differences in primary productivity (0.1 to 0.65 $gC/m^2/day$) in the modern ocean [Antoine *et al.*, 1996]. Today, potential temperatures estimated in the site locale at the water depth of 982 are 5 to 6 ºC [McCartney, 1992] suggesting the presence of an intermediate water, or Eastern North Atlantic Water (ENAW), delivering comparatively warmer waters to the high latitudes of the North Atlantic [Schmitz and McCartney, 1993; Andersson and Jansen, 2003]. The hydrographic conditions of today cannot be claimed as analogous to those during the Miocene-Pliocene sampling interval and we do not have core top calibrations for the nannofossil or BFAR data, however, some understanding of the hydrography is essential to the interpretation of results.

The nannofossil record at 982 is complete from the late Miocene through the Holocene (~18.8 to 0 Ma), though only the middle Miocene to early Pliocene sediments are examined for this project. The sampling is identical to that outlined in the design of Diester-Haass *et al.* [in press] which encompasses the ~6 myr long segment from ~9 to 3 Ma and has a temporal resolution for sampling aimed at ~40 kyr. Shipboard measurements conclude that these sediments are ~93 percent nannofossil ooze with chalk and minimal amounts of clay [Jansen *et al.*, 1996]. Of the ooze, ~91 percent is chalk from a well preserved assemblage of coccoliths [Jansen *et al.*, 1996]. The high carbonate content at Site 982 is important because data obtained by Stoll and Schrag [2000] shows adsorbed Ca and Sr cations from aluminosilicates within the nannofossil size fraction to affect the Sr/Ca ratio of a sample. The effect, however, is shown to decrease with increasing carbonate content [Stoll and Schrag, 2000]. This implies that high (over 80%) carbonate content within the sediments is necessary to obtain unambiguous results for nannofossil Sr/Ca and the sediments from Site 982 fit this criterion.

2.1.2 Ocean Drilling Program Site 925

ODP Site 925 is located on Ceara Rise in the western tropical Atlantic Ocean (Figure 1.1). The site lies just northeast of the Amazon River delta and is presently at a depth of approximately 3041 m (above the modern lysocline) where it is bathed by North Atlantic Deep Water (NADW) [Curry *et al.*, 1995; Tiedemann and Franz, 1997]. It is estimated, however, that water depths were probably 100 to 150 m shallower during the Miocene-Pliocene (like Site 982) [Andersson and Jansen, 2003].

Unlike Site 982, Site 925 is presently in a thermally stable environment and modern hydrography does not reveal significant differences in sea surface temperatures on a seasonal basis. There is, however, a slight shallowing of the thermocline and mixed layer depth during the winter months, bringing cool nutrient-rich waters slightly closer to the warm surface waters (Figure 2.1 B) [Levitus and Boyer, 1994]. Primary productivity also varies little on a seasonal basis (0.20 to 0.35 $gC/m^2/day$), but the annual average is the same as at Site 982 (12.5 $gC/m^2/day$) [Antoine *et al.*, 1996]; making this low latitude, warm water oligotrophic site a nice contrast (though comparable in average productivity) to ODP Site 982.

Site 925 contains a nannofossil record that is complete from the middle Eocene to the Holocene with abundant and generally diverse nannofossils in the middle Miocene to early Pliocene interval that is the focus of this project [Curry *et al.*, 1995]. The sediment from this site is classified as 60 to 85 percent nannofossil ooze and a combination of chalks and clays [Curry *et al.*, 1995]. Of this ooze, 85 to 95 percent is a diverse and well preserved assemblage of coccoliths and discoasters [Curry *et al.*, 1995]. Here again, the high carbonate content plays an important role in the minimization of aluminosilicates necessary to obtain clear results from the Sr/Ca record [Stoll and Schrag, 2000].

2.1.3 Ocean Drilling Program Site 926

With the publication of the Gibbs *et al.* [2004] study of nannofossil assemblage changes on Ceara Rise (ODP Site 926), an opportunity arose to examine species effects on size fractioned nannofossil Sr/Ca. The species counts published by Gibbs *et al.* [2004] provide a direct comparison between nannofossil species abundances and nannofossil

Sr/Ca. The close proximity of Site 926 to Site 925 may allow for the application of information gained about nannofossil Sr/Ca at this site to that at Site 925 (as assemblage components between the two, regardless of time scale, should be similar).

ODP Site 926 is located just about 50 km southwest of Site 925 on Ceara Rise (Figure 1.1) and contains a complete nannofossil record from the early Oligocene to the Holocene [Curry *et al.*, 1995], though this study focuses on the mid-Pliocene (~3.5 to 4 Ma) sediments. Here again the sediments at Site 926 consist primarily of alternating beds of nannofossil clays and ooze (resulting from dilution by terrestrial material) with carbonate contents varying between ~30 and 70 percent [Curry *et al.*, 1995].

Like Site 925, the location of Site 926 is northeast of the Amazon River delta, though it presently sits at approximately 3598 m depth (some 500+ m deeper than Site 925) [Curry *et al.*, 1995]. Site 926 is also bathed by North Atlantic Deep Water [Curry *et al.*, 1995; Tiedemann and Franz, 1997]. The location of Site 926 is above the modern carbonate lysocline, though some alteration (in the form of overgrown nannofossils and selective preservation of more dissolution tolerant species like *Discoaster* and *Calcidiscus*) is apparent in the sediments [Curry *et al.*, 1995; Gibbs *et al.*, 2004] and can be attributed to the deeper depth; despite this, the lithologic units as Site 926 and 925 are very similar [Curry *et al.*, 1995]. As the carbonate composition of the plates of coccoliths is homogenous, partial dissolution should not affect coccolith Sr/Ca in individual specimens [Stoll and Schrag, 2000]. This may, however, be complicated by the fact that individual species could contain distinct Sr/Ca signals and their selective dissolution would therefore alter the bulk coccolith record [Stoll and Schrag, 2000]. This issue further highlights the importance of monitoring species assemblages in conjunction with geochemical records.

2.2 Age models

Orbital scale age control is available for ODP Site 982. This is important for the calculation of sediment accumulation rates, and therefore the BFAR as derived from benthic foraminifera per gram of sediment. The age model for this site is based on the tuning of the benthic foraminiferal $\delta^{18}O$ record to obliquity [Hodell et al., 2001]. Because of this, the distribution of age control points at Site 982 is equal to or higher than the temporal resolution of this study, so the assumption that sedimentation rates between control points are constant and linear is likely a good one.

At ODP Site 925, the age model used is based on magnetic susceptibility as tuned to Northern Hemisphere summer insolation [Shackleton and Crowhurst, 1997; Diester-Haass *et al.*, in press]. Here again, the age control points are more densely distributed than the sample increments of this study. Consequently, the accumulation rates are assumed to be both constant and linear between control points.

The age model for Site 926 is that utilized by Gibbs *et al.* [2004]. Again, it is based on the tuning of the magnetic susceptibility record to Northern Hemisphere insolation as defined by Laskar [1990; Tiedemann and Franz, 1997]. This is further adjusted by tuning it to the astronomical solution, La1, and magnetic susceptibility maxima are tuned to target minima, assuming no lag [Gibbs *et al.*, 2004]. As no direct comparisons are being made between the sites, the utilization of differing age models amongst them is not a cause for concern.

2.3 Diagenesis

It is important to note that regions of high carbonate content, like those utilized here, can support diagenesis [e.g. Stout, 1985; Richter and Liang, 1993; Hampt-Andreasen and Delaney, 2000]. Diagenetic, or secondary inorganic, calcite is a cause for concern in all geochemical studies. In the case of nannofossil Sr/Ca, the presence of diagenetically altered calcite either on or within the plates will lower Sr/Ca values [e.g. Hampt-Andreasen and Delaney, 2000; Richter and Liang, 1993]. This is because the distribution coefficient of Sr in abiogenic calcite is fairly low in relation to that of biogenic calcite causing diagenetic calcite to be relatively Sr deplete [Carpenter and Lohmann, 1992]. In this regard, diagenetic alteration has the potential to uniformly reduce Sr/Ca (an advantage as the signals sought in this research are confined periods of increased ratios), but should not cause excursions in the records [e.g. Stoll and Schrag, 2001; Stoll and Bains, 2003].

In order to investigate the possibility of diagenetic alteration within the Site 982 and Site 925 samples, SEM viewing and imaging is employed. Diagenetic alteration of the nannofossils would tend to obscure the features of the plates and may result in the presence of euhedral crystal overgrowths on the calcite. SEM imaging of intervals from across the core from Site 982 reveals very well preserved coccoliths with no noticeable signs of overgrowth (Figure 2.2). Furthermore, when viewing the Site 982 samples under light microscopy, nannofossils are generally articulated and features well defined, a good sign that alteration of the samples is probably not a significant cause for concern [S. Gibbs, pers. comm.]; this supports the excellent preservation recorded in Shipboard Reports for this core [Jansen *et al.*, 1996]. SEM imaging of the Site 925 nannofossils reveals somewhat poorer nannofossil preservation than Site 982, as many of the features of the plates are obscured

(Figure 2.3). This less than pristine preservation is also present in smear slides of the samples which show specimens with visible signs of dissolution and disarticulation [S. Gibbs, pers. comm.]. No clear euhedral crystals overgrowths are apparent on the nannofossil faces, however, and Shipboard Reports classify the preservation of carbonate sediments in this region as well preserved [Curry *et al.*, 1995] suggesting that the effect of diagenetic alteration on the Sr/Ca ratios is minimal.

2.4 Size fractionation

One of the paramount concerns in geochemical studies involving nannofossils are the species effects, as the minute size of the fossils makes it difficult to utilize monospecific samples from the geologic record [e.g. Stoll and Ziveri, 2004]. Analyses by Stoll and Schrag [2000] suggest that in most instances, changes in the coccolith assemblage will probably not affect bulk coccolith Sr/Ca values on short time scales, though they caution that this may not hold true for shallow or species rich sediments or records over longer time scales [Stoll and Schrag, 2000]. Research shows that different nannofossil species may have substantial differences in Sr/Ca [Stoll *et al.*, 2002b; Stoll and Bains, 2003; Stoll and Ziveri, 2004; H. Stoll, pers. comm.]. Therefore, as species abundances wax and wane and even appear and disappear entirely, the Sr/Ca values of bulk sediments may be affected.

ODP Site 982 offers the distinct advantage, as a result of its hydrographic and ecologic setting, of containing comparatively limited nannofossil species diversity (Table 2.1). Taking this and the exploratory nature of the investigation into account, only the bulk nannofossil Sr/Ca is measured at Site 982. With the understanding that species richness at the tropical Ceara Rise Site 925 is enhanced (in comparison to Site 982) the methods and

approach to analysis are altered to include a size fractionation step aimed at putting partial constraints on the nannofossil assemblages.

This idea is further tested by the addition of nearby ODP Site 926 with a known assemblage and nannofossil abundances that ultimately guided the selection of size fractionation criterion [Gibbs *et al.*, 2004; S. Gibbs, pers. comm.]; with the objective being to split the species into groupings of smaller and larger plate sizes to be able to better constrain species effects. Specifically, the intent exists to cleanly isolate the discoasters in the coarse fraction, and the selected split size also makes for a fairly nice ecological division of the species. The fractionation divides the cooler water, mesotrophic species into the fine fraction and the warmer, more oligotrophic taxa into the coarse fraction, with few exceptions (e.g. *Reticulofinestra haqii* and *Sphenolithus abies* which may be present in both the fine and coarse size fractions; Table 2.2) [S. Gibbs, pers. comm.].

2.5 Foraminiferal geochemistry

2.5.1 Sr/Ca and seawater

Given that the distribution coefficient of Sr in calcite is directly related to the Sr/Ca of the medium within which it is formed, it follows that secular changes in the Sr/Ca of seawater [e.g. Stoll and Schrag, 2001; Lear *et al.*, 2003] would affect nannofossil Sr/Ca. That having been said, the major sources of Sr to the oceans are primarily limited to river input and hydrothermal activity and the residence times of Sr are quite high in terms of geologic time (5.1 myrs) [Broecker and Peng, 1982]. The data collected by Stoll and Schrag [2000] shows much more pronounced fluctuations in coccolith Sr/Ca than those in foraminifera Sr/Ca, from which they conclude that the nearly 15% variation observed in coccolith Sr/Ca

must result from changes in Sr partitioning within the coccolith carbonate, rather than just fluctuations in seawater Sr/Ca (which varied by less than 2%) [Stoll and Schrag, 2000].

To account for this possible seawater influence, synchronous records of planktonic foraminiferal (*Globigerinoides sacculifer* at Site 925 and *Globigerina bulloides* at Site 982) Sr/Ca are generated to parallel the nannofossil Sr/Ca records. As changes in seawater chemistry (e.g. seawater Sr/Ca and carbon chemistry) would affect the planktonic foraminifera and nannofossils in the same way, similar fluctuations in the two records can be assumed to result from changes in the seawater. Hence, variations unique to the nannofossil Sr/Ca are assumed to show some control on Sr partitioning (ie. calcification, growth rate and/or productivity).

2.5.2 Mg/Ca and temperature

Given that studies [e.g. Stoll *et al.,* 2002b] indicate that temperature may also play a role in the distribution of Sr into the coccolith, temperature effects cannot be ruled out in nannofossil Sr/Ca analysis. A definitive stance has not yet been taken on this issue, however, as the nature of the relationship is complex and there are many difficulties faced in separating the sea surface temperature effects and those of increased calcification resulting from warmer temperatures and more ideal growth conditions.

Planktonic foraminiferal Mg/Ca, measured simultaneously with the Sr/Ca discussed previously, provide an opportunity to monitor mixed layer paleotemperatures. At the very least, the Mg/Ca record should demonstrate whether or not large climate related temperature fluctuations occur during the time interval of investigation. However, as the calcification habitat of the foraminifera studied does not necessarily overlap with the

calcification environment of the nannofossils, a direct correlation between foraminiferal Mg/Ca and nannofossil Sr/Ca is not sought here.

2.5.3 Foraminiferal diagenesis and contamination

As discussed earlier, diagenetic alteration of biogenic carbonate can pose a problem for geochemical studies, so the preservation of the planktonic foraminifera used for analysis must also be evaluated. As a result of the higher distribution coefficient of magnesium in diagenetic calcite (in relation to biogenic calcite), Mg/Ca ratios are actually increased during diagenesis (where Sr/Ca ratios are lowered) [Carpenter and Lohmann, 1992]. This is to say that there may be a relationship between low Sr/Ca values and high Mg/Ca values in diagenetically altered calcite. A plot was made of Sr/Ca versus Mg/Ca for the *G. sacculifer* planktonic foraminiferal data (Figure 2.4 shows the data from Site 925; data for Site 982 are currently being generated) to assess diagenetic alteration. There is no noticeable association of low Sr/Ca and high Mg/Ca for this plot so it can be assumed that diagenesis is not an obvious concern. Additionally, contamination within foraminifera samples can also be a problem and may be indicated by high Mn/Ca. To this extent, Mn/Ca obtained for the *G. sacculifer* show no major outliers, and all values fall below one, suggesting that contamination it not a concern in this data set (refer to Appendix C for *G. sacculifer* Mn/Ca measurements). While these diagnostics can not rule out the possibility of poorer sediment preservation affecting the signals in the sediments, they do suggest that the geochemical signature has been retained.

Chapter 3

EXPERIMENTAL METHODS

3.1 Slide and stub production for viewing and imaging

In order to view the nannofossils via scanning electron microscopy (SEM), the samples are prepared and placed on stubs in accord with methods used by H. Stoll [pers. comm.]. A portion of the cleaned (procedures to follow in Section 3.2.1) and dried nannofossil fraction is diluted in a 2% ammonia solution to inhibit aggregation and the solution is further diluted and sonicated briefly until it is no longer milky in color, though a series of varying dilutions is ultimately used. This solution is then pipetted into a syringe filtering set up and filtered through a 0.45 μm cellulose nitrate filter. The filter itself is allowed to dry and a punch is used to acquire smaller discs of filter which are mounted on aluminum SEM stubs with double-sided carbon adhesive stickers (see Appendix A for complete procedure description). The samples are kept in a desiccator prior to viewing on the Hitachi field emission scanning electron microscope (FE-SEM) in the Delaware Biotechnology Institute's facility at the University of Delaware.

Additionally, a series of samples are prepped for viewing and analysis via light microscopy. Smear slides are made following a series of basic steps as supplied and instructed by S. Gibbs [pers. comm.]. To begin, a cover slip is licked and then a small amount of the cleaned nannofossil fraction is scraped onto the slip. One drop of deionized

(DI) water is then added to the slip and a toothpick is used to disaggregate and smear the sediment. Once a satisfactory distribution of varying sample density is obtained across the slip, the slip is heated on a hot plate to remove the excess moisture. Two drops of Norland Optical Adhesive are placed on the middle of a labeled slide, and the cover slip is placed (sediment side down) on top of the adhesive. The slide is placed back on the hot plate to allow the adhesive to liquify and spread evenly between the slide and cover slip, and the slide is then set on a windowsill so that the UV radiation can harden the adhesive (see Appendix A for a complete description of smear slide production methods). The samples are viewed both on site and within the Geology Department at Penn State University with a Zeiss petrographic microscope primarily under cross polarized light.

3.2 Nannofossil processing

3.2.1 Nannofossil Sr/Ca cleaning

The majority of the lab work for this research involves the cleaning and preparation of sediment samples for analysis. The samples for all of the ODP sites are archived bulk fine fraction sediments. Each of the 95 samples from the middle Miocene to early Pliocene unit of the core from Site 982, 89 samples from the middle Miocene to early Pliocene unit of the Site 925 core and the 67 samples from the middle Pliocene unit of the Site 926 core were processed to isolate the nannofossil fraction from the remainder of the sediments and ensure that the Sr/Ca values obtained are from the nannofossils and not foraminiferal carbonate or contamination. The cleaning of the samples for analysis is done with a modified version of the methods developed and refined by H. Stoll and her colleagues [Apitz, 1991; Bairbakesh *et al.*, 1999; Stoll and Schrag, 2000; Stoll and Ziveri, 2002; H. Stoll, pers. comm.].

To begin the cleaning process, approximately 0.100 g to 0.150 g of bulk sediment is weighed out and wet sieved through a 20 μm copper sieve with ethanol in order to remove any foraminifera or foraminiferal fragments. The sediment which passes through the sieve is reacted and sonicated in a sodium hypochlorite and hydrogen peroxide solution to oxidize the organic matter, disaggregate the sediment and remove any non-carbonated metals [Bairbakesh *et al.*, 1999]. The recovered sediment is vacuum filtered through a 0.8 μm polycarbonate filter, resuspended, centrifuged and isolated again. This recovered fraction is then reacted with an "MNX" [after Stoll and Schrag, 2000; H. Stoll, pers. comm.] solution of hydroxylamine hydrochloride, ammonium hydroxide and DI water to reduce the Fe-Mn oxy-hydroxides that scavenge metals from seawater [Apitz, 1991]. Repeated reacting and decanting of the recovered sediment with the ammonium oxide and DI water solution, "IONX" [after Stoll and Schrag, 2000; H. Stoll, pers. comm.], removes adsorbed strontium and further disperses the nannofossils [Apitz, 1991]. For Site 982, the remaining chalk is allowed to dry before 200 μg fractions are weighed out and quartered (the samples from Site 925 and 926 require further processing which will be described in Section 3.2.2). Please refer to Table 3.1 for a step by step description of the procedure.

3.2.2 Size fractionation

Once the nannofossil chalk has been cleaned, reacted and decanted twice in the "IONX" solution (following the methods laid out in Table 3.1), each of the samples from Sites 925 and 926 is split into fine (0.8 to 8.0 microns) and coarse (8.0 to 20.0 microns) size fractions. In order to do this, each sample is resuspended in a weak ammonium hydroxide and water solution. They are then slowly vacuum filtered through a series of 8.0 μm

polycarbonate filters in order to avoid clogging. The fine fraction which passes through the filters is transferred into a vial, allowed to settle overnight and then centrifuged. The remaining solution is pipetted away and the samples are allowed to dry. The coarse fraction which remains on the filter is transferred to a vial using DI water and centrifuged before the solution is pipetted away and the samples allowed to dry. Once dry, 200 μg of the coarse nannofossil chalk is weighed out and quartered by eye. One of these quarters is transferred to a vial for analysis and the remaining is archived for future use.

3.3 Planktonic foraminiferal minor element cleaning

The Sr/Ca of planktonic foraminifera was measured for synchronous intervals of the cores to constrain variations that are unique to the nannofossils. As the general long term trend is the crucial element, approximately every other interval (of the original sample sets) for Site 925 and 982 was used for this analysis resulting in 40 to 50 data points for each. Foraminifera from the samples had been washed and sorted by size prior to receipt. At Site 982, the samples are sieved in the 250 to 355 micron range and 20 to 24 specimens of the planktonic foraminifera, *Globigerina bulloides*, are picked. For the Site 925 samples, sieving is conducted in the 355 to 425 micron range and 12 to 16 specimens of the planktonic foraminifera, *Globigerinoides sacculifer*, are picked. The foraminifera are briefly sonicated in DI water, oven dried and weighed. After weighing, the foraminifera are crushed between two clean glass plates, and a subsample (50 to 350 μg and 300 to 600 μg, respectively) is weighed out and placed in a vial for minor element cleaning.

The minor element fraction of crushed foraminiferal carbonate is subjected to a standard protocol cleaning process (without the reductive step) like that utilized by Brown

and Elderfield [1996], Lear *et al.* [2000] and discussed by Rosenthal *et al.* [2004]. The method is designed to minimize sample loss, yet ensure that all of the chemical treatments are rinsed away from the sample. Like that used for the cleaning of nannofossils for Sr/Ca analysis, this cleaning procedure follows a series of steps aimed at the removal of clays and oxidation of organic matter (refer to Table 3.2 for a detailed description of methods).

3.4 Sample analysis

All of the cleaned nannofossil bulk, coarse and fine fractions, as well as the crushed foraminifera are dissolved in 2% trace metal grade nitric acid prior to analysis to obtain a concentration of ~100 ppm for each sample. Trace element analysis of the samples occurred at the University of Oxford's inductively coupled plasma mass spectrometry (ICP-MS) facility using the PerkinElmer PESCIEX ELAN 6100 DRC Quadrupole ICP-MS (Q-ICPMS). Each sample is bracketed by two standards and corrections are made for both matrix effects and long term drift. The analytical precision over 9 months using a 100 ppm standard is better than 0.6% for Sr/Ca and 0.7% for Mg/Ca.

Chapter 4

RESEARCH RESULTS

4.1 Seawater Sr/Ca

The minor element analysis of *Globigerinoides sacculifer* from ODP Site 925 in the subtropical Atlantic (results of the *Globigerina bulloides* analysis from Site 982 are pending) yields Sr/Ca values nearly identical to those from DSDP Site 588 in the South Pacific (Figure 4.1) [Scheiderich, 2004]. Both records reveal relatively little variability in Sr/Ca, with an average at about 1.2 mmol/mol. While there is a very slight increase in the records from approximately 1.1 mmol/mol at ~8.5 Ma to about 1.3 mmol/mol at ~3.5 Ma, there do not appear to be any systematic fluctuations in Sr/Ca over the course of the interval. Consequently, any changes in the nannofossil Sr/Ca superimposed over this long term trend are not likely to be the result of seawater Sr/Ca as they would also be recorded in the planktonic foraminifera. For Site 926, the short time interval investigated (~210 kyr; much shorter than the ~5 Ma and ~1 Ma residence time of Sr and Ca, respectively) is more than enough reason to preclude the need for a record of seawater Sr/Ca. Therefore, all data reported here will be reported in terms of nannofossil Sr/Ca in mmol/mol, rather than the distribution coefficients for strontium.

4.2 Ocean Drilling Program Site 982

The Sr/Ca record from Site 982, although measured on the entire size fraction, shows a gradual increase from ~8 to 4 Ma (Figure 4.2 A). Superimposed on this long term trend is a shift to lower Sr/Ca values between ~7.5 and 7.0 Ma. Also, there is a more notable increase beginning at ~5.6 Ma with a pronounced maximum at 4.7 Ma.

The long term trend observed in the nannofossil Sr/Ca measurements is consistent with those seen in the BFAR and $CaCO_3$, which show a gentle rise in what is assumed to be productivity, towards more recent times. However, the absolute magnitude of the gradual long term trend in Sr/Ca may in part reflect increasing seawater Sr/Ca ratios (as judged by the Sites 925 and 588 planktonic foraminifera). This aside, there is a distinct maximum present at approximately 5 Ma in the nannofossil Sr/Ca values, as well as the other records (Figure 4.2). This maximum in the nannofossil Sr/Ca appears to follow that in the other records slightly, reaching its peak at ~4.8 Ma.

When comparing the small scale trends of the nannofossil Sr/Ca records and BFAR records of paleoproductivity, a number of the individual maxima and minima are remarkably similar. This includes the periods from ~8.9 to 6.5 Ma and ~5.9 to 4.5 Ma (Figure 4.2 A and B). Also noteworthy are similarities in the degree of variability across the records; for each of the proxies, fluctuations in the observed values are highest during the interval surrounding the productivity maxima (~5.5 to 4.5 Ma). The degree of variance of measured values for LSR and $CaCO_3$ are likewise high around these intervals (Figure 4.2 C and D, respectively). On the other hand, the lowest degree of variability in both the nannofossil Sr/Ca and BFAR records occurs around 6.75 to 6.25 Ma. Here again, LSR and $CaCO_3$ reveal a lack of variability like those seen in the nannofossil Sr/Ca and BFAR at this time.

4.3 Ocean Drilling Program Site 925

The results for the fine and coarse fraction nannofossils at Site 925 also show a long term trend of gradually increasing Sr/Ca ratios from ~8 to 4 Ma (Figure 4.3 A) that is likely due in part to increasing seawater Sr/Ca. There is a clear separation of Sr/Ca measurements between the coarse and the fine fractions with the coarse fraction having generally higher ratios. The coarse fraction Sr/Ca range from ~1.5 mmol/mol to ~2.5 mmol/mol, while the majority of the fine fraction ranges from ~1.0 to ~2.3 mmol/mol. Given that these fractions are taken from the same samples, the varying Sr/Ca levels are likely the result of assemblage differences between the two fractions [e.g. Stoll et al., 2002b; Stoll and Bains, 2003]. Additionally, variability, resulting mainly from peak maxima values, appears to be greater in the fine fraction nannofossils (~1.0 to 2.3 mmol/mol at the outset) than the coarse fraction (~1.6 to 2.4 mmol/mol) across this interval of time. The single point peaks in the fine fraction nannofossil Sr/Ca approach the observed coarse fraction values (e.g. those at ~7.4 Ma, 6.9 Ma, 5.7 Ma, 5.3 Ma, 5.1 Ma and 4.2 Ma). This may be consistent with some degree of contamination of the fine fraction by broken portions of the larger species not being captured in filtering (a possibility presently under investigation).

The coarse fraction coccolith Sr/Ca values appear to have relatively little variability (Figure 4.3 A). Visible in the long term trend is a marked maximum towards the end of the record, at ~4.3 Ma. Also of note is the change in the amplitude of variability across the interval (even though it is still small relative to the finer fraction), with Sr/Ca measurements ranging from about 1.6 and 1.8 mmol/mol from ~8.3 to 7 Ma and then increasing in variability with intervals of lesser degrees of variability like that from ~5.6 to 5.2 Ma.

The fine fraction Sr/Ca record from Site 925 illustrates a prominent increase in nannofossil Sr/Ca from ~6.8 to 5.9 Ma with a distinct maxima at ~6.3 Ma outlined by a series of increasing and then decreasing data points (Figure 4.3 A). Clear minima are missing during this period of heightened Sr/Ca in comparison to the remainder of the section. There also appears to be a decrease in fine fraction Sr/Ca around 4.2 Ma just before values rise again through the end of the record.

On the smaller scale, some good agreement is found between individual maxima and minima from ~7.5 to 5.9 Ma (including, though not limited to, maxima at approximately 7.4 Ma, 6.9 Ma, 6.4 Ma and 5.9 Ma and minima at approximately 6.8 Ma, 6.5 Ma, 6.3 Ma, 6.2 Ma and 6.0 Ma; Figure 4.3). This interval encompasses the clearly evident maxima in the fine fraction, and careful examination does reveal a minor maximum, though quite well muted, in the coarse fraction. The last million years of the two records demonstrates substantial disagreement, as the coarse fraction is marked by a distinct maximum and the fine fraction a considerable minimum in Sr/Ca values suggesting that species effects may be preserved within the fractionated Sr/Ca.

Comparison of the nannofossil fine fraction Sr/Ca observations to the LSR, $CaCO_3$ and BFAR records of Diester-Haass *et al.* [in press] reveals good agreement (Figure 4.3 A, E, D and C respectively). In particular, the increase in fine fraction Sr/Ca between ~6.7 and 6.0 Ma, as well as the maxima at ~6.4 Ma is synchronous with the maxima in BFAR and also agrees well with high values of $CaCO_3$ and LSR. The records of Diester-Haass *et al.* [in press] also show a slight increase in values at ~4.8 Ma. Outlying values of fine fraction Sr/Ca (determined by the fact that they exceed even the coarse fraction Sr/Ca) keep this maximum from being resolved in the nannofossil records, however, this may be indicative of

an increase in and of itself (duplicates for these samples are being generated). On the shorter scale, relatively good peak to peak agreement can also be found between the fine fraction nannofossil Sr/Ca and BFAR records from ~7.5 to 5.8 Ma (including maxima at ~7.4 Ma, 6.9 Ma, 6.7 Ma, 6.45 Ma, 6.15, 6.05 Ma and minima at ~7.5 Ma, 6.8 Ma, 6.4 Ma, 6.2 Ma, 6.1 Ma and 5.9 Ma). While some of the fine fraction maxima do suggest that there may be a mixing of species between fractions, the timing of the increased nannofossil Sr/Ca measurements and tight variability does agree well with the individual BFAR peaks at the same intervals suggesting the presence of an environmental signal.

The minor element analysis of *G. sacculifer* from Site 925 yields Mg/Ca values ranging between ~3.2 and 4.7 mmol/mol (Figure 4.4 A). The overall long term trend in the data begins with a very slight decrease from ~8.4 to 7.4 Ma followed by a sharp rise in values which begin to fall at ~6.9 Ma. Mg/Ca climbs from ~6.8 to 6.6 Ma where it remains relatively high before falling off again from ~6.3 to 6.0 Ma. The measurements climb very gradually until about 5.7 Ma where they plateau and remain steady until approximately 4.8 Ma. This is followed by a steady decline in Mg/Ca from ~4.7 to 4.1 Ma, and relatively variable measurements through the end of the record at ~3.8 Ma. The increase and then decrease measured in *G. sacculifer* Mg/Ca values between 6.7 and 6.0 Ma roughly parallels the record of enhanced productivity depicted by the fine fraction nannofossil Sr/Ca (Figure 4.4 A and B) and BFAR. As *G. sacculifer* is a mixed layer dweller this suggests that near surface water temperatures also have changed during this period. However, as this is the only example where the temperature and productivity records appear to be related, this implies that it is not a temperature effect on calcification rate. Instead, this may be an expression of a climatic link between productivity and temperature.

4.4 Ocean Drilling Program Site 926

At ODP Site 926, the size fractionated nannofossil Sr/Ca records are generated for comparison to the high resolution nannofossil species counts of Gibbs *et al.* [2004]. Gibbs *et al.* [2004] find that the abundances of a few species of nannofossil, including *Sphenolithus*, *Florisphaera profunda* and total *Discoasters* vary with insolation and inversely with magnetic susceptibility (Figure 4.5 A, B, C and D).

The minor element nannofossil measurements generated for Site 926 are similar to those of Site 925 in that the Sr/Ca of the size fractions are distinct and the coarse fraction values (~1.8 to ~2.6 mmol/mol) are higher than those of the fine fraction (~1.6 to ~2.1 mmol/mol) (Figure 4.5 E). Although similar in these ways, the records are different in that it is the coarse fraction which varies and appears to be demonstrating a climatic signal (Figure 4.5 E). This is most likely a function of the higher resolution of the Site 926 analyses suggesting that insolational fluctuations in the Site 925 coarse fraction nannofossils may be masked by aliasing and that the long term trends in the fine fractions at Site 926 are not captured because of the shortened time frame under examination.

A cyclic pattern is clearly evident in the coarse fraction nannofossil Sr/Ca data, but not the fine fraction (Figure 4.5 E). Minima are found in the coarse fraction record at approximately 3.865 Ma, 3.835 Ma, 3.815 Ma, 3.785 Ma, 3.760 Ma, 3.740 Ma and 3.150 Ma. This pattern nearly parallels that of insolation, inversed magnetic susceptibility, *Sphenolithus*, *F. profunda* and *Discoaster* abundances [Figure 4.5]. However, since *Sphenolithus* (a species whose abundance drops off midway through the interval) and *F. profunda* are both smaller nannofossil species which are contained predominantly within the fine fraction, the *Discoasters* (a large species and major contributor to the coarse fraction assemblage) will be

the focus of discussion to follow. Low Sr/Ca values are found to coincide with minimal *Discoaster* abundances [Gibbs *et al.*, 2004], minima in the record for insolation of Laskar [1990] and maxima in magnetic susceptibility [Gibbs *et al.*, 2004].

Chapter 5

DISCUSSION

5.1 Overview

The results of these analyses show that over the long term, agreement is present between the nannofossil Sr/Ca and BFAR proxies for productivity, and records of surface ocean productivity covary with consumption at the seafloor through significant intervals of time suggesting that a link does exist between the two processes. The Sr/Ca values at both ODP Sites 982 and 925 show an increase at approximately the same time as the BFAR measures of paleoproductivity. This connection is promising and supports an increase in paleoproductivity, associated with nannoplankton production, during the late Miocene–early Pliocene interval. In particular, because the increase in proxy values is not concurrent at Site 982 and 925, but is between the different proxy records at each site, it further highlights the presence of a link between the top down and bottom up perspectives on productivity (as opposed to some other factor effecting both reconstructions) and suggests regional changes and controls on hydrography. While the following discussion focuses on the links found between records over the course of this research, some concession must be made as there are aspects of the data which will require further analysis and investigation to fully understand.

5.1.1 ODP Site 982

The results from ODP Site 982 support a paleoproductivity increase at ~5 Ma. This is indicated by the maximum peaks in nannofossil Sr/Ca, BFAR and $CaCO_3$. The timing of this increase is consistent with the results of Grant and Dickens [2002] which show increases in carbonate mass accumulation rates in the western subtropical Pacific at this time. Also, this agrees well with the Indian Ocean $CaCO_3$ MARs of Peterson *et al.* [1992] and reconstructions of paleoproductivity from the Tasman Plateau [Diester-Haass and Nees, 2004] further supporting the evidence for a globally synchronous increase in productivity at this time. Diester-Haass *et al.* [in press] suggest that the synchronicity of records further highlights the potential existence of a global increase in nutrients in the late Pliocene and the results of this research suggest the presence of a nannofossil bloom.

There is a discrepancy in the timing of the absolute maxima for the various proxies. As noted above, the peak observed in nannofossil Sr/Ca values at about 4.8 Ma is about 20 kyr younger than the maxima in the other records. Given the number of uncertainties associated with both the Sr/Ca and BFAR proxies and the complex nature of the transport of sediments from the photic zone to deep, the presence of even general agreement between the records is encouraging and suggests that there is some link between surface ocean productivity and accumulation rates at depth. The offset in records could potentially be clarified by higher resolution sampling that should produce a more coherent data set. The increase in nannofossil Sr/Ca supports the idea of enhanced calcification, which further supports increased $CaCO_3$ accumulation.

5.1.2 ODP Site 925

The results of the investigation of the Ceara Rise core from ODP Site 925 also show good agreement between proxies. The late Miocene–early Pliocene interval at Site 925 clearly indicates that a considerable portion of the fine fraction nannofossil Sr/Ca values are in very good agreement with BFAR and $CaCO_3$ records. All of the proxies show increased measurements at ~6.3 Ma supporting an increase in paleoproductivity in the late Miocene–early Pliocene, as well as implying a link between surface ocean primary productivity, in the form of nannofossil Sr/Ca, and deep ocean consumption as BFAR. Signals seen within both the geochemical and accumulation rate records offer a convincing argument for increased productivity in the geologic record.

In contrast to the good agreement seen between fine fraction nannofossil Sr/Ca and the other records for productivity, the coarse fraction Sr/Ca measurements for the interval at Site 925 do not show any notable similarities with the other proxies on this long time scale. This may suggest that species specific controls by the larger taxa have masked the signal in the coarse fraction. Another possibility, which will be built upon in the discussion to follow, is that the coarse fraction varies on a time scale not captured here and, therefore, may not be especially effective at demonstrating productivity fluctuations in the long term. These results seem to suggest that microfiltering for size fractionation of the nannofossils [e.g. Stoll and Bains, 2003; Stoll, 2005] could play a critical roll in the geochemical analyses of nannofossils and this idea could be tested further through complete assemblage monitoring of both the fine and coarse size fractions across the interval.

5.1.3 ODP Site 926

At Site 926 it was possible to test for the effect of species fluctuations directly using the samples and species counts provided by Gibbs *et al.* [2004]. The results of the Sr/Ca analysis in this instance are surprising in that the high resolution coarse fraction nannofossils appear to be the ones telling the story (unlike those at Site 925). Here, cyclic patterns of the coarse fraction Sr/Ca are in phase with insolation, as well as *Discoaster* abundances and reversed magnetic susceptibility [Gibbs *et al.*, 2004]. Low Sr/Ca for the coarse fraction is coincidental with low *Discoaster* counts, depicting nearly parallel trends. The fine fraction Sr/Ca record does not possess these same characteristics suggesting that at these shorter time scales, the discoasters are either setting or responding to the variations, unlike the long time scale results of Site 925 which show changes in the fine fraction. Essentially, this would imply that the *Discoaster* variations are obscured at Site 925 because of the low resolution sampling, and that the high resolution at Site 926 is too short of a record to show the long term fluctuations.

The *Discoasters*, an extinct genus of carbonate producing nannoplankton, exhibit strong cyclic variation in abundance during the study interval [Gibbs *et al.*, 2004]. This is not the first occasion on which such patterns have been found in *Discoaster* counts; Late Pliocene *Discoaster* records also show similar patterns [e.g. Backman *et al.*, 1986; Backman and Pestiaux, 1987; Chepstow-Lusty *et al.*, 1989]. While the discoaster flora are not very well understood, they are thought to be warm water (as their distribution is consistent across lower latitudes) species [e.g. Haq and Lohmann, 1976; Lohmann and Carlson; 1981; Chepstow-Lusty *et al.*, 1989, 1991; Flores *et al.*, 1995, 2005] and as such, may record temperature variations over time [e.g. Backman *et al.*, 1986; Backman and Pestiaux, 1987].

Work by Chepstow-Lusty *et al.* [1989] and Chapman and Chepstow-Lusty [1997], however, demonstrates higher amplitude fluctuations in abundance that can not solely be explained by temperature, suggesting they also appear to be oligotrophic, and the body of literature seems to agree that discoaster abundances can be inhibited by both decreasing temperature and increasing nutrient availability.

Based on the agreement between the total *Discoaster* abundances and coarse fraction Sr/Ca records at Site 926, two scenarios (or a combination of them) may explain the cyclicity in the records. One, assuming that discoasters dominate the coarse fraction (conversion of counts to carbonate contribution is necessary and in progress) and that Sr/Ca is determined by calcification rate and/or growth, high Sr/Ca during a time of high *Discoaster* abundance is consistent with conditions favorable for the genus (warm oligotrophic waters). Then, as hydrographic conditions become less ideal for discoasters, they do not calcify as much and/or as rapidly and therefore have lower Sr/Ca. This implies that discoaster productivity is actually driving the coarse fraction Sr/Ca variations observed in the 926 record.

Florisphaera profunda abundances bear mentioning for this first scenario as they exhibit similar cyclic variations to the *Discoaster* abundances and coarse fraction Sr/Ca. Though they are not contained within the coarse size fraction, *F. profunda* abundances have been used quite extensively in the Quaternary as a proxy for productivity [e.g. Molfino and McIntyre, 1990; McIntyre and Molfino, 1996; Beaufort *et al.*, 1997, 2001; Bassinot *et al.*, 1997] and therefore serve as supporting evidence for the cyclic productivity fluctuations seen in the coarse fraction Sr/Ca. In the geologic record, *F. profunda* is found to be relatively abundant where shallow dwelling taxa are low and surface waters are deprived of nutrients as a result of its relationship with light intensity [Okada and Honjo, 1973; Ziveri *et al.*, 1995;

Cortés *et al.*, 2001; Haidar and Thierstein, 2001]. This and the alternate conditions, low abundances of *F. profunda* in combination with a shallow thermocline and high nutrient availability is the foundation on which the proxy is based [Molfino and McIntyre, 1990]. For the Site 926 abundance data, *F. profunda* is found to exhibit cyclic variations similar to those in *Discoaster* and coarse fraction Sr/Ca, where abundance maxima are associated with low magnetic susceptibility implying once again that there might be a localized nutrient driven signal (Figure 4.5 A) [Gibbs *et al.*, 2004]. This further supports the nannofossil Sr/Ca record and, in combination with the *Discoaster* abundances, suggests that there may have been a common productivity mechanism acting on Ceara Rise nannofossils in the mid-Pliocene.

Despite this evidence, it is not possible to rule out the second scenario for the paralleling records from nannofossils at Site 926. This scenario suggests that the variations in coarse fraction Sr/Ca indicate, at least in part, that discoaster ratios are generally consistently high and as there numbers decrease, other species with lower ratios begin to dominate the assemblage. This means that the proportions of nannofossils within the assemblage would be the primary mechanism by which the sediment Sr/Ca is controlled. Without individual species measurements of Sr/Ca (and in particular that of discoasters) this is not easy to confirm.

In order for the *Discoasters* to be influencing the Sr/Ca signal in this scenario, they would have to have a characteristic Sr/Ca value which is higher than other species within the fraction. In this regard, the data collected here do not necessarily agree with the published literature which has shown coarse fractions and discoaster containing carbonate to have typically lower Sr/Ca values [Stoll and Bains, 2003; H. Stoll, pers. comm.]. This contradiction, however, could be explained by species variation, on both a temporal and

spatial scale. The Stoll and Bains [2003] study examined Paleocene-Eocene Thermal Maximum coarse fraction (8.0 to 12.0 μm) carbonate from the Weddell Sea with possible species including *Discoaster anartios*, *araneus*, *diastypus*, *lenticularis*, *mahmoudii*, *mohleri*, *multiradiatus*, and *salisburgensis* [Bralower, 2002]. In the mid-Pliocene Site 926 coarse fraction (8.0 to 20.0 μm) sediments, *Discoaster* species include *assymetricus*, *brouweri*, *pentaradiatus*, *surculus*, *tamalis*, and *variabilis* [Gibbs *et al.*, 2004]. While relatively little is known about discoasters as they are extinct, given the distinction seen in the Sr/Ca of size fractionated assemblages like those reported here it is not unrealistic to expect different species with dissimilar sizes to possess differing Sr/Ca levels across the geologic time scale. Additionally, nannofossil measures of Sr/Ca in the Paleocene-Eocene interval are generally lower (~0.8 to 1.8 mmol/mol) [Stoll and Bains, 2003] than those observed in the Miocene-Pliocene sediments (1.0 to 2.6 mmol/mol; consistent with gradually rising seawater Sr/Ca over time) and therefore, a direct comparison of the results of these studies is difficult.

The fact that the total *Discoaster* abundances at Site 926 are at their minima in association with high magnetic susceptibility and low insolation (Figure 4.5 B, C and D) supports the interpretation that, on orbital time scales, discoaster abundances (and perhaps calcification and/or growth) may be suppressed by increased nutrient availability and/or decreased temperatures. According to Gibbs *et al.* [2004], this shows that orbitally driven terrigenous supply from the Amazon River to the Ceara Rise, possibly coupled with increased organic matter and nutrients, may be affecting water transparency and ultimately exerting a strong local control on productivity and *Discoaster* abundances.

Another possibility exists for this orbital forcing in these sediments, however, and that is related to surface hydrography [Gibbs *et al.*, 2004] and the depth of the thermocline.

Given what is known about the variation in thermocline depth on a seasonal basis in this region, it might also be expected that thermocline depth would be affected by fluctuations in insolation. Work by Niemitz and Billups [2005] show that surface water hydrography (and in particular thermocline and mixed layer depth) respond to insolational forcing during the early Pliocene at ODP Site 925. That is to say that during periods of insolation maxima (Northern Hemisphere), there would also be strong monsoonal circulation over North Africa which would weaken the south easterly trade winds causing pile up of warm waters along the western coast of the Atlantic (and specifically in the region of Ceara Rise) [Mix *et al.*, 1995; Niemitz and Billups, 2005]. This would result in a relatively deep thermocline and warm nutrient poorer waters within the photic zone, while the opposite scenario (insolation minima and strengthened south easterly trade winds) would minimize pile up, yielding a shallower thermocline depth and more nutrient availability in the photic zone. Given this scenario, the nannofossil assemblage could be responding to insolation driven fluctuations in thermocline depth and their effect on temperature and nutrient availability rather than an external signal [K. Billups, pers. comm.; Gibbs *et al.*, 2004].

5.2 Paleoclimate during the Miocene-Pliocene

The results of this research provide geochemical evidence for intervals of increased paleoproductivity in the Atlantic Ocean during the late Miocene to early Pliocene which is concurrent with other productivity proxies like BFAR. While the exact mechanisms for this increase are unknown, possible means of forcing include the onset of more idealized surface water temperature conditions and/or increased nutrient input (a factor that may also be related to warming temperatures), both of which could be associated with uplift and

enhanced weathering of the Himalayan plateau [e.g. Filippelli, 1997] and/or an initiation and intensification of the Asian monsoonal system [e.g. Filippelli, 1997; Gupta and Thomas, 1999; Hermoyian and Owen, 2001]. All of these modes could provide a means for increased calcification of coccolithophorids and the subsequent increases in nannofossil Sr/Ca. Regardless of the cause, there is good evidence for similar responses around the globe. Overall, it appears as though this study interval possesses an intriguing climatic forcing mechanism and continued research will be required to resolve the causes of the increases as well as the relationships amongst them. The foregoing research emphasizes the presence of a link between surface ocean productivity as captured by nannofossil Sr/Ca and deep ocean consumption in the form of BFAR; further suggesting that top down geochemical proxies for paleoproductivity, like Sr/Ca, may be used to fill in some of the gaps in the geologic record left by other productivity proxies that are inhibited by age model and sedimentation rate assumptions.

Chapter 6

SUMMARY AND CONCLUSIONS

6.1 Paleoproductivity proxy evaluation

This research set out with the primary intent of comparing productivity proxies in an effort to better understand the limitations of the various proxies as well as the connections, if any, between them. As such, the examination of nannofossil Sr/Ca records for productivity and those produced from benthic foraminiferal accumulation rates (BFAR) seem to yield promising results. Generally speaking, good agreement is seen between the two proxy records at both ODP Site 982 and 925; of particular note is the increase seen in BFAR and bulk Sr/Ca around 5 Ma at Site 982, as well as, the Site 925 increases in observed BFAR and fine fraction Sr/Ca that are synchronous at ~6 Ma. Overall, the data suggests that some link does exist between the two proxy records, implying coupling between primary production at the ocean surface, export production, and consumption along the seafloor.

The inconsistencies observed between the BFAR and Sr/Ca data in other intervals, like the offset in Sr/Ca around 4.8 Ma at Site 982 or the differing variation between coarse and fine fraction Sr/Ca at Site 925, suggest that there are still aspects of these reconstructions which we do not understand. Species counts on the bulk sediments from Site 982 and size fractions from Site 925 would provide information on the nannofossil assemblage fluctuations in the reconstructions which may shed some light on the causes of

divergence between these records. Higher resolution analyses of the Site 925 core and a lengthened time interval of study at Site 926 could also contribute significantly to the interpretation of these Ceara Rise productivity reconstructions.

While the major complication for accumulation rate paleoproductivity proxies, like BFAR and $CaCO_3$, is the bias produced by their dependence on sedimentation rates, and this makes independent geochemical proxy signals (like those in nannofossil Sr/Ca) very appealing, it would seem they come with their own set of concerns. Continued research is necessary to gain a better understanding of temperature and species effects on nannofossil Sr/Ca. Higher resolution sampling and strict monitoring of down core assemblages may allow for a more unequivocal interpretation of such reconstructions. The underlying theme appears to be that resolving past fluctuations in productivity will require the combination of multiple productivity proxy measurements (offering the most potential where the observations are collected from one set of samples, or synchronous intervals) and the continued collaboration and cooperation of scientists from across the spectrum, from sedimentologists and geochemists to micropaleontologists and biologists.

6.2 Miocene-Pliocene biogenic bloom

Assuming that the nannofossil Sr/Ca records generated at ODP Sites 982 and 925 are guided primarily by productivity and not other factors, like temperature (though it cannot be unequivocally ruled out), the data collected over the course of this project do support the idea of increased productivity in late Miocene to early Pliocene interval, as well as the existing body of evidence [e.g. Peterson et *al.*, 1992; Grant and Dickens, 2002; Diester-Haass and Nees, 2004; Diester-Haass *et al.*, in press]. While the recorded maxima at Site 982 (~4.8

Ma) and Site 925 (~6.3 Ma) are neither synchronous nor equitable in length, regional and climatic forces may be expected to play a role in the distribution of an ocean, if not world-wide, 'biogenic bloom'. Regardless of the forcing or controlling factors on sizeable increases in productivity at this time, the data supports the existence of a mechanism which appears to be able to produce a signal in both the geochemical and sediment accumulation rate records.

6.3 Direction for future work

The research presented here raises many interesting questions and provides a basis for continued studies of paleoproductivity, the proposed late Miocene-early Pliocene biogenic bloom, and orbital forcing in nannofossil paleoclimate records. In particular, through this study it has become apparent that interpreting paleoproductivity reconstructions is an extremely complex undertaking. It appears that unlocking the productivity stories housed in the geologic archive will be best accomplished by the integration of many different proxies for productivity and that measuring multiple parameters within synchronous sediment samples is the best approach.

One possible suggestion for the continuation of this research is in the production of complete species abundance counts for the ODP Site 982 and 925 cores in order to compare to the nannofossil Sr/Ca measures. Additionally, a higher resolution sampling may reveal cyclic patterns (like those at Site 926) which have been masked by aliasing in the Site 925 sediments. Also, it may help to develop and implement improved size fractionation methods utilizing three-way size splits specific to the assemblages to ensure a more definitive separation of species [e.g. Stoll and Bains, 2003; Stoll, 2005]. At the same time, a comparison of nannofossil Sr/Ca and alkenone biomarker records for coccoliths [see Stoll

and Ziveri, 2004 for an overview] within the core might help to establish whether or not the variation seen in the observed Sr/Ca values for the cores may be associated with sea surface temperatures, and consequently whether or not a temperature effect is present in the data.

The most promising aspect of this study and the primary direction to pursue appears to be the continued development of the mid-Pliocene nannofossil record from ODP Site 926. With the assistance of S. Gibbs, a list of dimensions and shape factors is being compiled for the various species present in the core and this will be used to convert the species abundance counts to carbonate contribution for comparison with the nannofossil Sr/Ca records. Additionally, extending the record, perhaps further back into the early Pliocene and even Miocene may reveal the presence of long term trends like those seen at Site 925 and may offer a significant contribution to our understanding of Miocene-Pliocene oceanography along Ceara Rise. In either regard, further investigation should help paint a clearer picture of insolar forcing in the lower latitudes during the Pliocene as well as factors affecting the nannofossil Sr/Ca in this region during that interval of time.

Table 2.1: All nannofossil species present in the Miocene-Pliocene assemblage at ODP Site 982 in the North Atlantic [S. Gibbs, pers. comm.].

Bulk nannofossil species (0.8 to 20.0 microns)
Amaurolithus delicatus
Amaurolithus primus
Calcidiscus leptoporus
Calcidiscus macintyrei
Calcidiscus tropicus
Coccolithus pelagicus
Discoaster asymmetricus
Discoaster quinqueramus
Discoaster surculus
Discoaster tamalis
Discophaera tubifera
Gephyrocapsa
Pseudoemiliania lacunosa
Reticulofenestra pseudoumbilica
Scyphosphaera apsteinii
Syracosphaera pulchra

Table 2.2: Some, though not all, nannofossil species separated by size fractionation of the Miocene-Pliocene assemblage at ODP Sites 925 and 926 in the tropical Atlantic [S. Gibbs, pers. comm.].

Fine fraction nannofossil species (0.8 to 8.0 microns)	**Coarse fraction nannofossil species (8.0 to 20.0 microns)**
Calcidiscus leptoporus	*Calcidiscus macintyrei*
most *Calcidiscus tropicus*	large *Calcidiscus tropicus*
most *Coccolithus pelagicus*	large *Coccolithus pelagicus*
Florisphaera profunda	*Discoaster asymmetricus*
Gephyrocapsa	*Discoaster blackstockiae*
small *Helicosphaera*	*Discoaster brouweri*
Oolithus	*Discoaster pentaradiatus*
many *Pontosphaera*	*Discoaster surculus*
most *Pseduoemiliania*	*Discoaster tamalis*
Reticulofenestra haqii	*Discoaster triradiatus*
Reticulofenestra minuta	*Discoaster variabilis*
small *Reticulofenestra pseudoumbilicus*	large *Helicosphaera*
small *Sphenolithus abies*	large *Reticulofenestra pseudoumbilicus*
Syracosphaera pulchra	*Rhabdosphaera*
Thoracosphaera fragments	*Scyphosphaera apsteinii*
Umbilicosphaera sibogae	*Scyphosphaera globulata*
Umbilicosphaera jafari	*Scyphosphaera intermedia*
Umbilicosphaera rotula	*Scyphosphaera lagena*
	Scyphosphaera pulcherrima
	Scyphosphaera tubifera
	large *Sphenolithus abies*
	Thoracosphaera

Table 3.1: Nannofossil Sr/Ca cleaning methods employed for this research. Methods are a modified version of those adapted and utilized by Stoll and Schrag [2000] and Stoll and Ziveri [2002] [H. Stoll, pers. comm.].

STEP	PROCESS	PURPOSE
I	Wet sieve 100 - 150 mg bulk sediment through 20 μm sieve using a soft brush and ~12 ml ethanol. Transfer to 15 ml tube, centrifuge and pipette away ethanol.	Separates foraminifera and foraminiferal fragments from nannofossil fraction.
II	To sieved fraction, add 2 ml DIH_2O, 2 ml 6% ClHO, and 2 ml 30% H_2O_2; react in tube for 1 hr, adding 1 ml 3% ClHO and sonicating for 15 sec every 15 min. Vacuum filter (.8 μm cellulose nitrate), recovering sediment on filter and resuspend in ~12 ml DIH_2O; centrifuge and pipette away liquid (reddish) x2.	Oxidizes organic matter, aids in the disaggregation of sediments and removes non-carbonated metals.
III	To sieved fraction, add 5 ml "MNX" (5 g hydroxylamine hydrochloride, 40 ml NH_4OH, 15 ml DIH_2O) in hood; react ~12 hrs on shaker table, centrifuge and pipette away liquid.	Reduces Fe-Mn oxy-hydroxides that scavenge metals from seawater.
IV	To sieved fraction, add 5 ml "IONX" (6.5 ml NH_4OH, 100 ml DIH_2O); react 12 - 24 hrs on shaker table, centrifuge and pipette away liquid.	Removes adsorbed Sr and acts as a dispersant.
V	To sieved fraction, add 5 ml "IONX" (see above); react for 12 - 24 hrs on shaker table, centrifuge, pipette away liquid and let dry; weigh ~200 μg, quarter and transfer one quarter (~50 μg) to 15 ml tube.	Repeated decanting; preparation for dissolution.
VI	Dissolve separated fraction in trace metal grade 2% HNO_3 (sonicate and mix thoroughly), subsampling 2 ml for analysis; archive the remaining.	Dissolves sample for analysis.

Table 3.2: Foraminiferal minor element cleaning methods used for this project. Procedure is a modified version of the Boyle Method for trace-metal cleaning.

STEP	PROCESS	PURPOSE
I	Place minor element split of crushed foraminifera in vial.	
II	Sonicate sample in DIH_2O and pipette away liquid. Sonicate sample in methanol for 1 min and pipette away. Fully rinse vial with DIH_2O and pipette away. Sonicate sample in DIH_2O and pipette away x2. Remove all liquid with pipette before continuing on.	Removes clays.
III	Sonicate sample in 250 μl NH_4Cl for 1 min and pipette away liquid. Fully rinse vial with DIH_2O and pipette away. Sonicate sample in DIH_2O and pipette away x2. Remove all liquid with pipette before continuing on.	
IV	Use water bath on hot plate to heat sample in 250 μl H_2O_2/NaOH solution (100 μl H_2O_2, 30 ml 0.1M NaOH) for 5 min with vials capped. Remove from bath, sonicate briefly, and heat for 5 more min before pipetting away liquid. Fully rinse vial with DIH_2O and pipette away. Sonicate sample in DIH_2O and pipette away x2. Remove all liquid with pipette before continuing on.	Oxidizes and removes organic matter.
V	Briefly sonicate in 250 μl .01M HNO_3 and let settle. Fully rinse vial with DIH_2O and pipette away liquid. Sonicate sample in DIH_2O and pipette away x4. Leave small amount of DIH_2O in vial on final rinse.	Minimizes possible contamination.
VI	Transfer remaining DIH_2O and sample to a clean and dry vial with pipette. Remove nearly all DIH_2O and cap vial for shipping.	Eliminates chemical transfer.

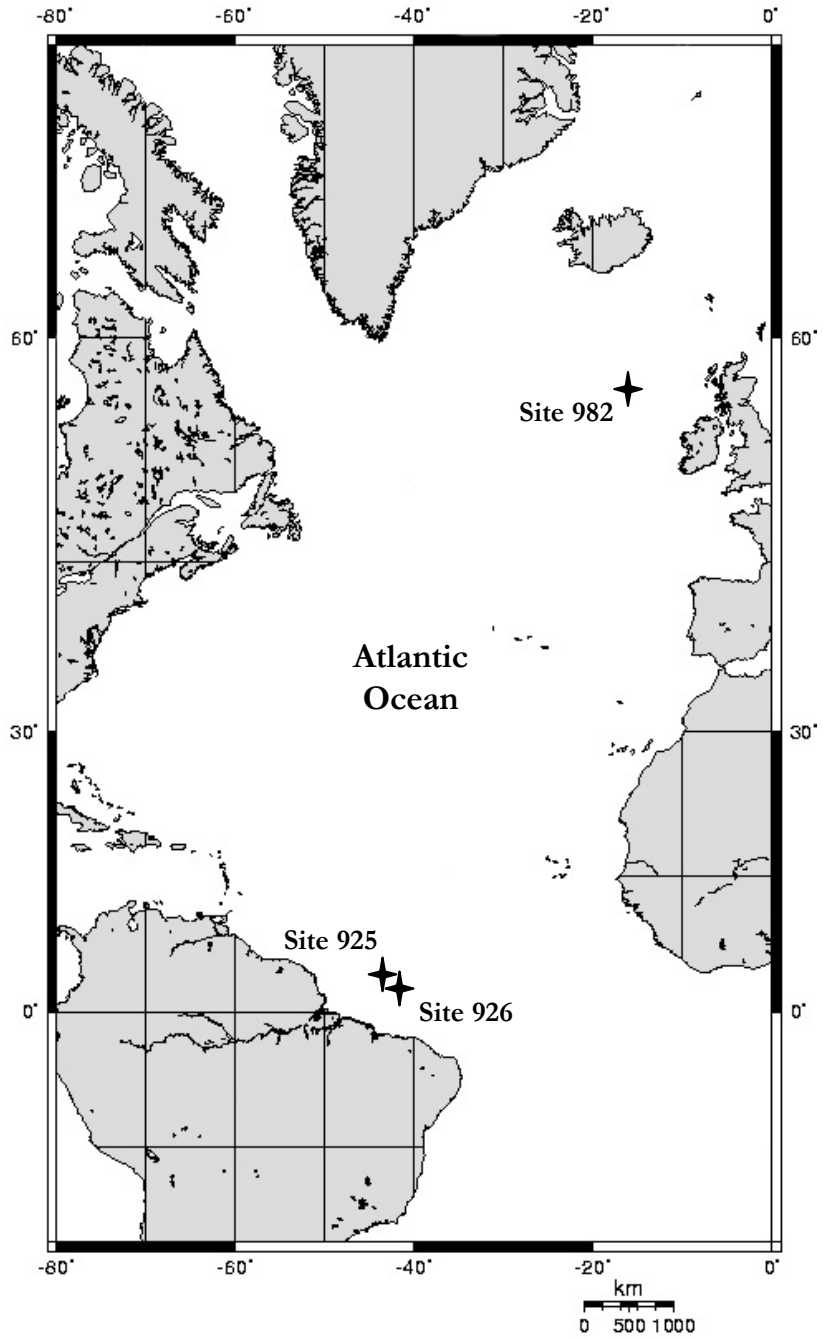

Figure 1.1: Mercator map projection of the Atlantic Ocean indicating the locations of ODP sites studied in this thesis, including Sites 982 (57°31'N; 15°52'W), 925 (4°12'N; 43°29'W) and 926 (3°43'N; 42°54'W). Map generated using Online Map Creation (OMC).

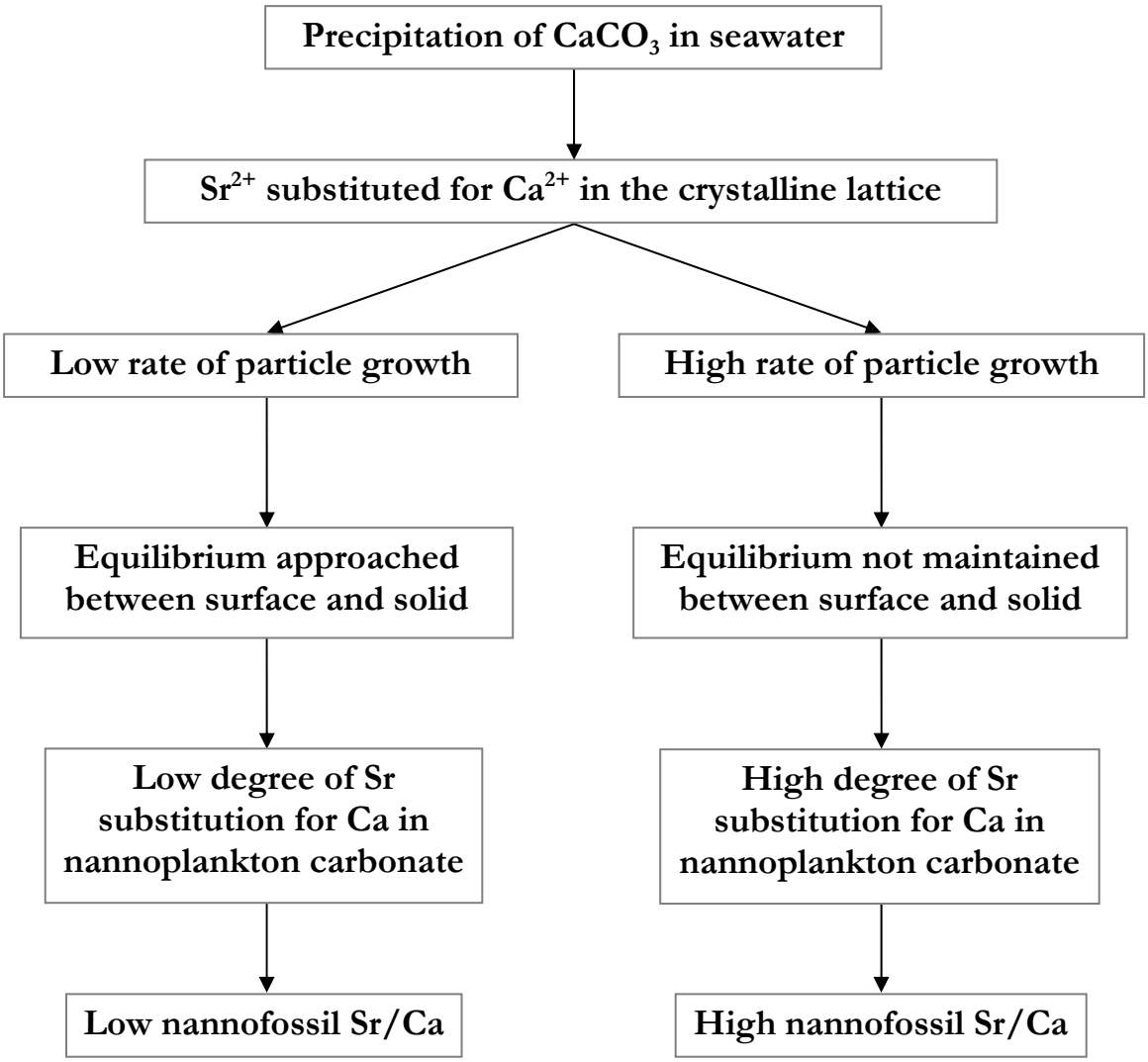

Figure 1.2: Flow chart depicting the possible kinetic mode by which Sr may be incorporated into nannofossil carbonate plates. Note that other more biogeochemical oriented controls are also suspected to regulate nannofossil Sr/Ca.

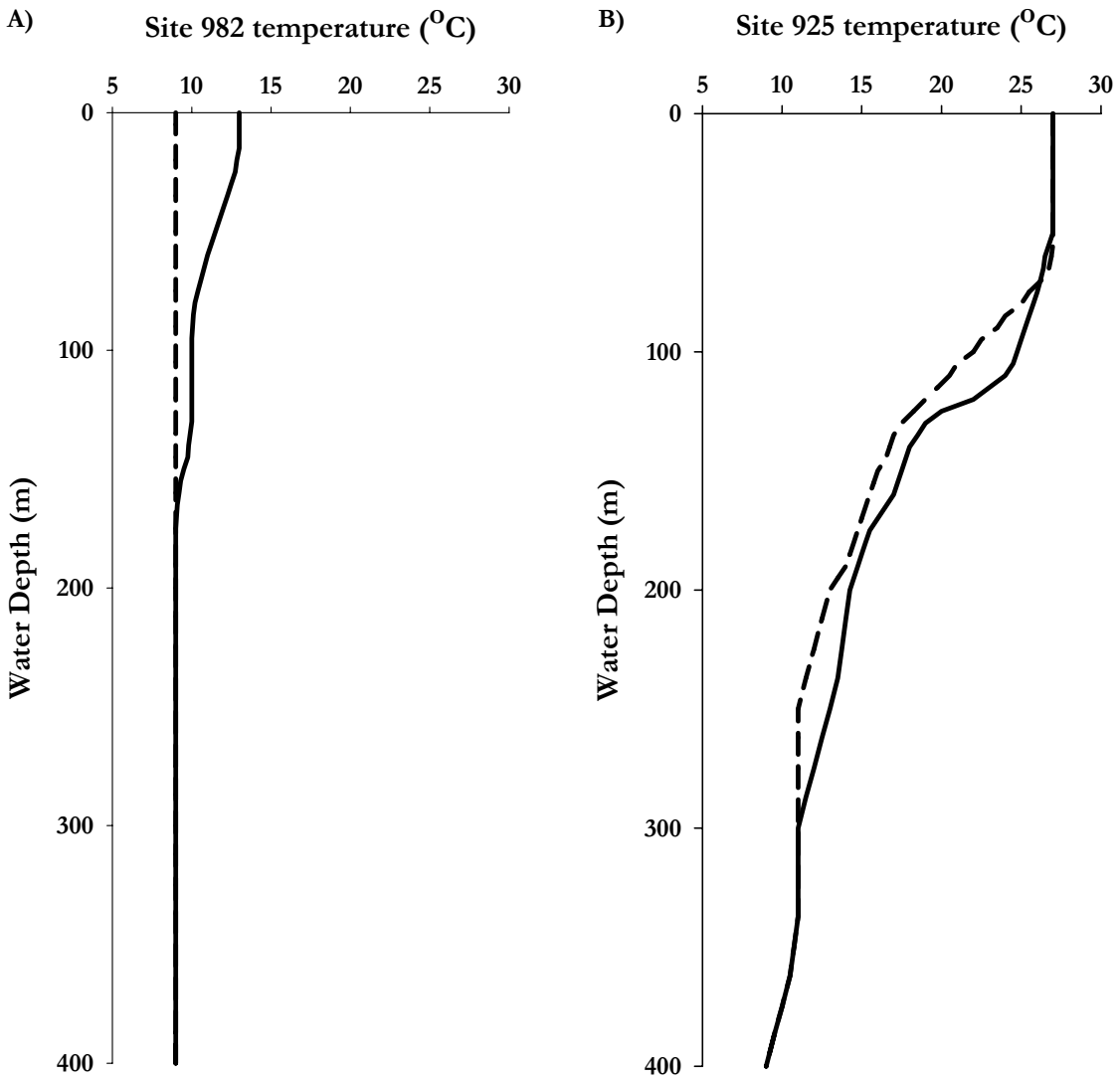

Figure 2.1: Estimated modern day temperature profiles for ODP Sites A) 982 and B) 925 from Levitus and Boyer [1994] data. Winter profile (dashed line) represents January through March and summer profiles (solid line) July through September. Plots generated utilizing the online International Research Institute and Lamont Doherty Earth Observatory (IRI/LDEO) Climate Data Library.

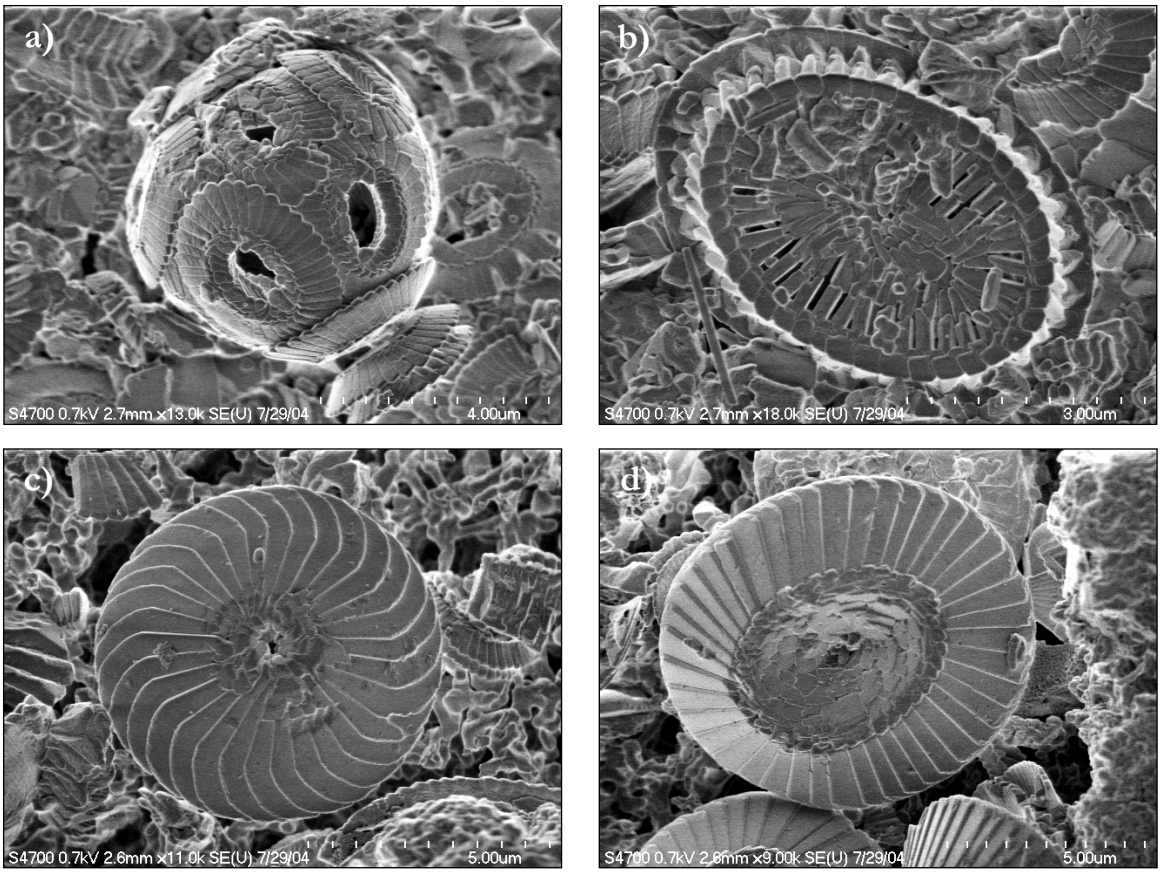

Figure 2.2: Scanning electron microscopy (SEM) images of processed coccoliths from ODP Site 982 in the North Atlantic including a) *Coccolithus pelagicus* coccosphere (sample 9H-5 53-55), b) *Syracosphaera pulchra* (sample 9H-5 53-55), c) *Calcidiscus leptoporus* (sample 19H-4 71-73), d) *Coccolithus pelagicus* (sample 19H-4 71-73). The individual calcite platelets appear well preserved with no visible signs of secondary calcification.

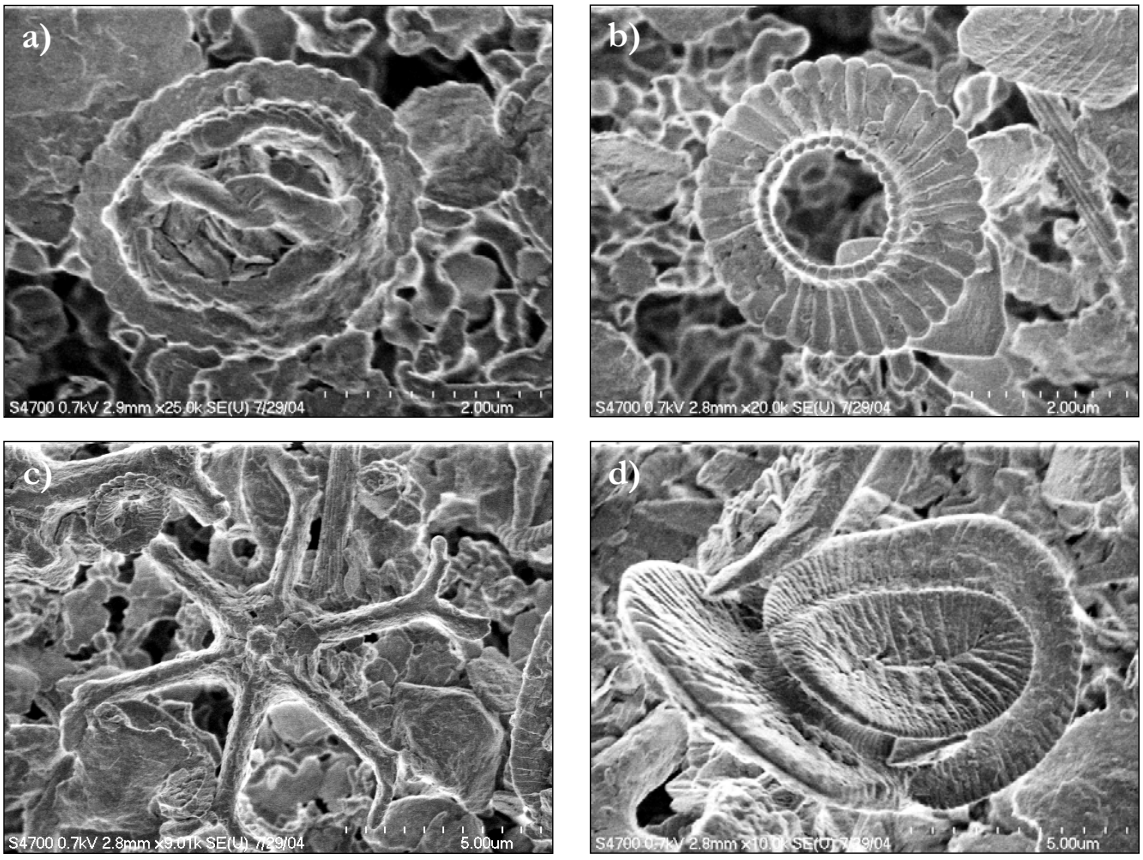

Figure 2.3: Scanning electron microscopy (SEM) images of processed nannofossils from ODP Site 925 in the tropical Atlantic including a) *Gephyrocapsa sensii* (Gibbs *et al.*, 2004) disarticulated shield (sample 13H-3 93-95), b) *Umbilicosphaera sp.* disarticulated shield (sample 17H-7 58-60), c) *Discoaster variabilis* (sample 17H-7 58-60), d) *Helicosphaera carteri* (sample 22H-4 51-53). The individual calcite platelets are relatively well preserved with no apparent euhedral crystals.

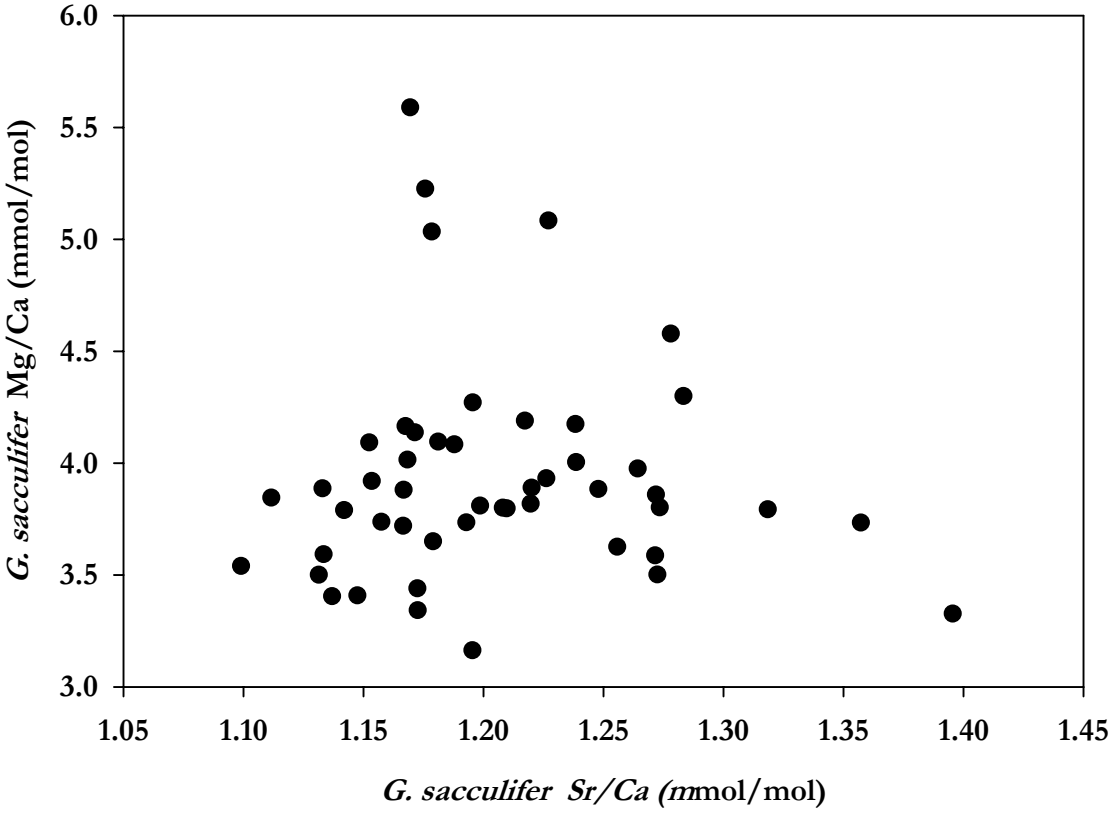

Figure 2.4: ODP Site 925 planktonic foraminifera *Globigerinoides sacculifer* Sr/Ca (mmol/mol) plotted versus Mg/Ca (mmol/mol) measurements collected simultaneously via Q-ICPMS.

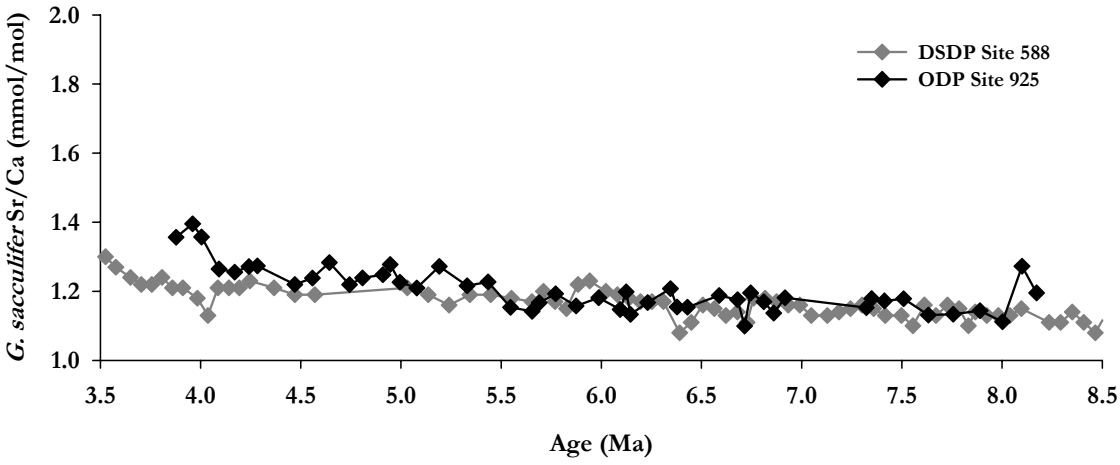

Figure 4.1: ODP Site 925 and DSDP Site 588 [Scheiderich, 2004] *Globigerinoides sacculifer* Sr/Ca (mmol/mol) plotted versus age for study interval.

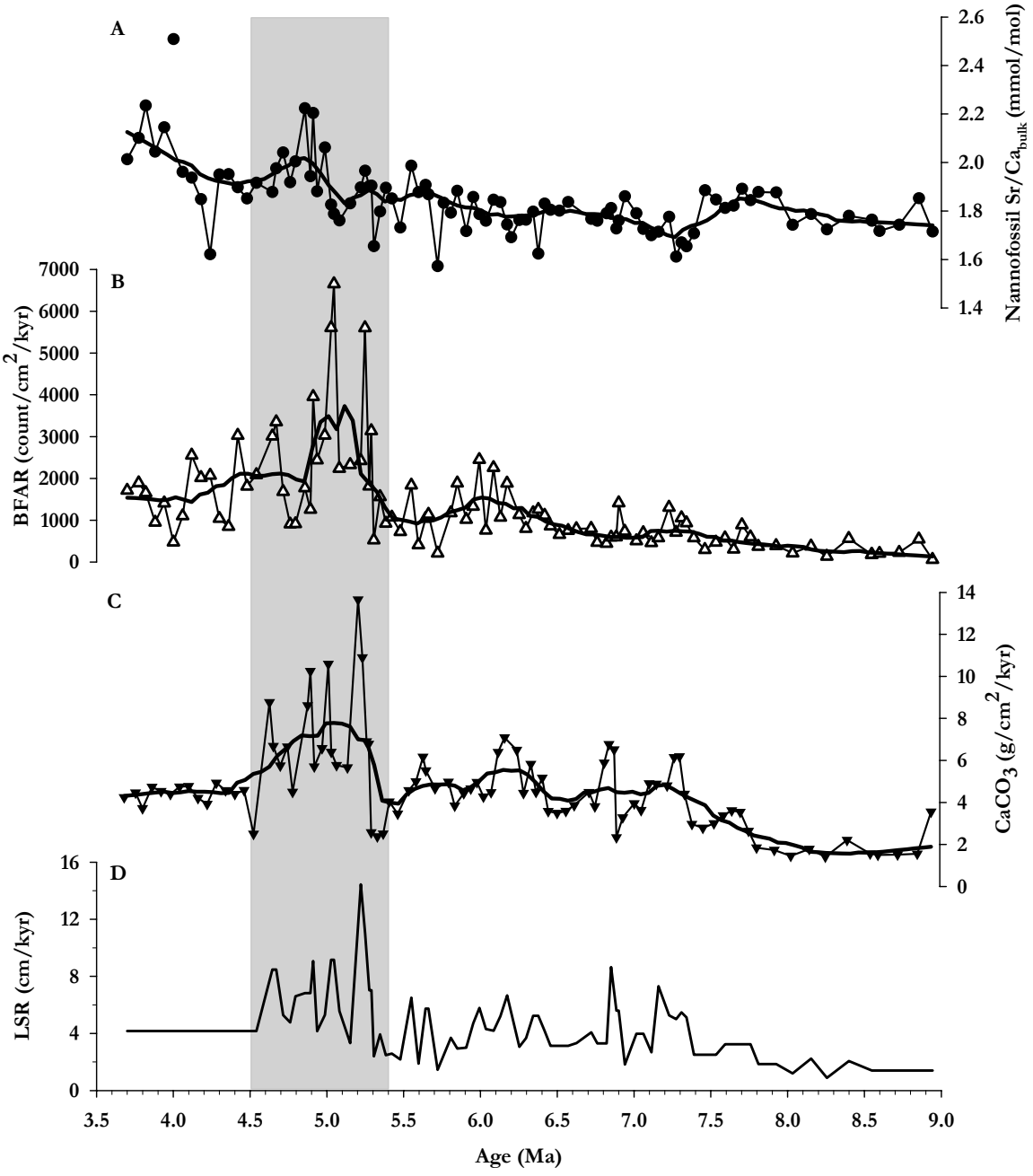

Figure 4.2: ODP Site 982 paleoproductivity records: A) bulk nannofossil Sr/Ca (mmol/mol) measured during this project, B) BFAR (count/cm^2/kyr), C) $CaCO_3$ (g/cm^2/kyr) and D) LSR (cm/kyr) from Diester-Haass *et al.* [in press]. Singular data point is likely an outlier and therefore not used to highlight the long term trend as expressed by the smoothed (10% exponential function) bold line.

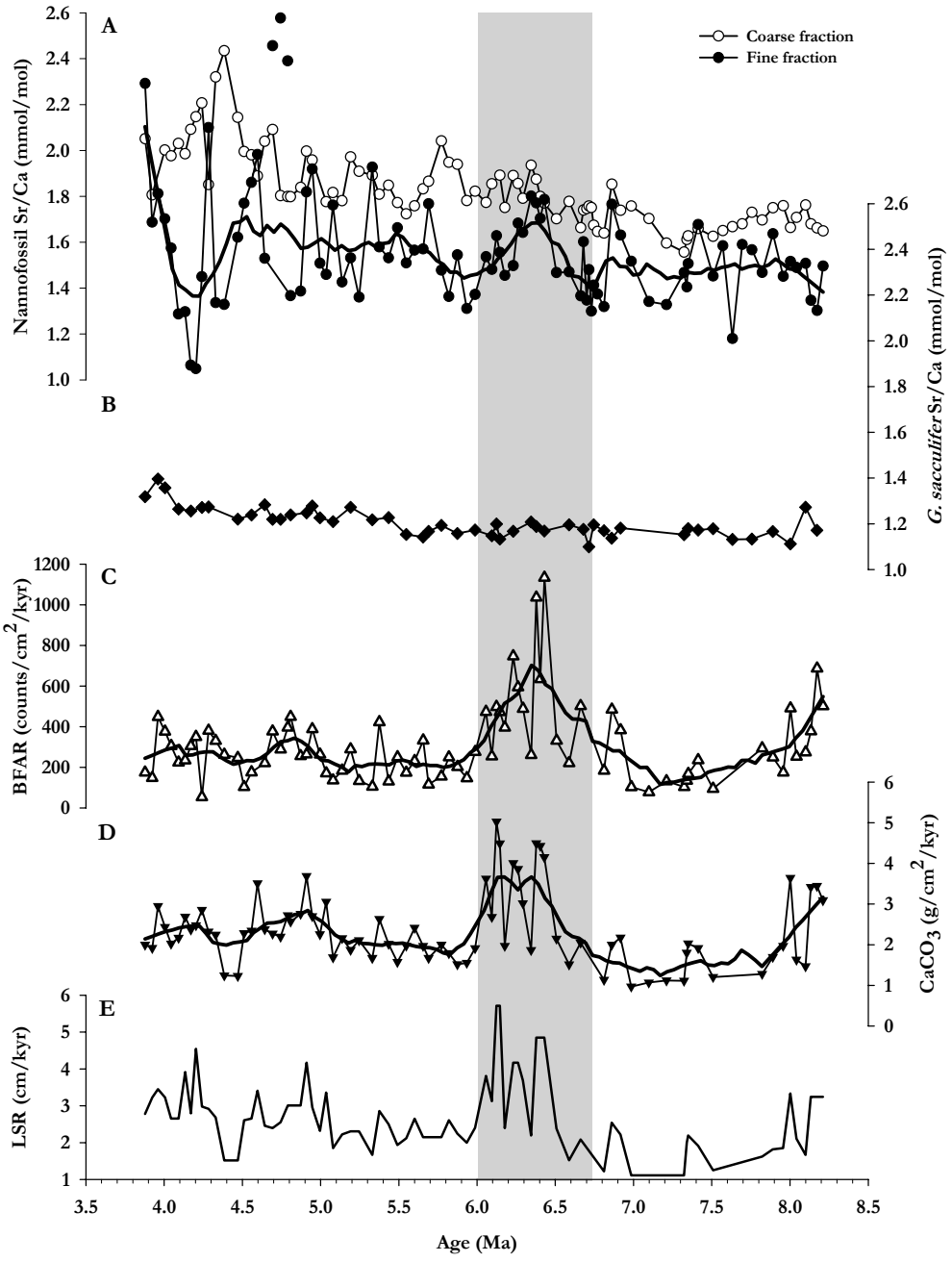

Figure 4.3: ODP Site 925 paleoproductivity records: A) coarse and fine fraction nannofossil Sr/Ca (mmol/mol) measured during this project, B) *Globigerinoides sacculifer* Sr/Ca (mmol/mol) also measured during this project, C) BFAR (count/cm^2/kyr), D) $CaCO_3$ (g/cm^2/kyr) and E) LSR (cm/kyr) from Diester-Haass *et al.* [in press]. Singular data points are likely outliers and therefore not used to highlight the long term trend as expressed by the smoothed (10% exponential function) bold line.

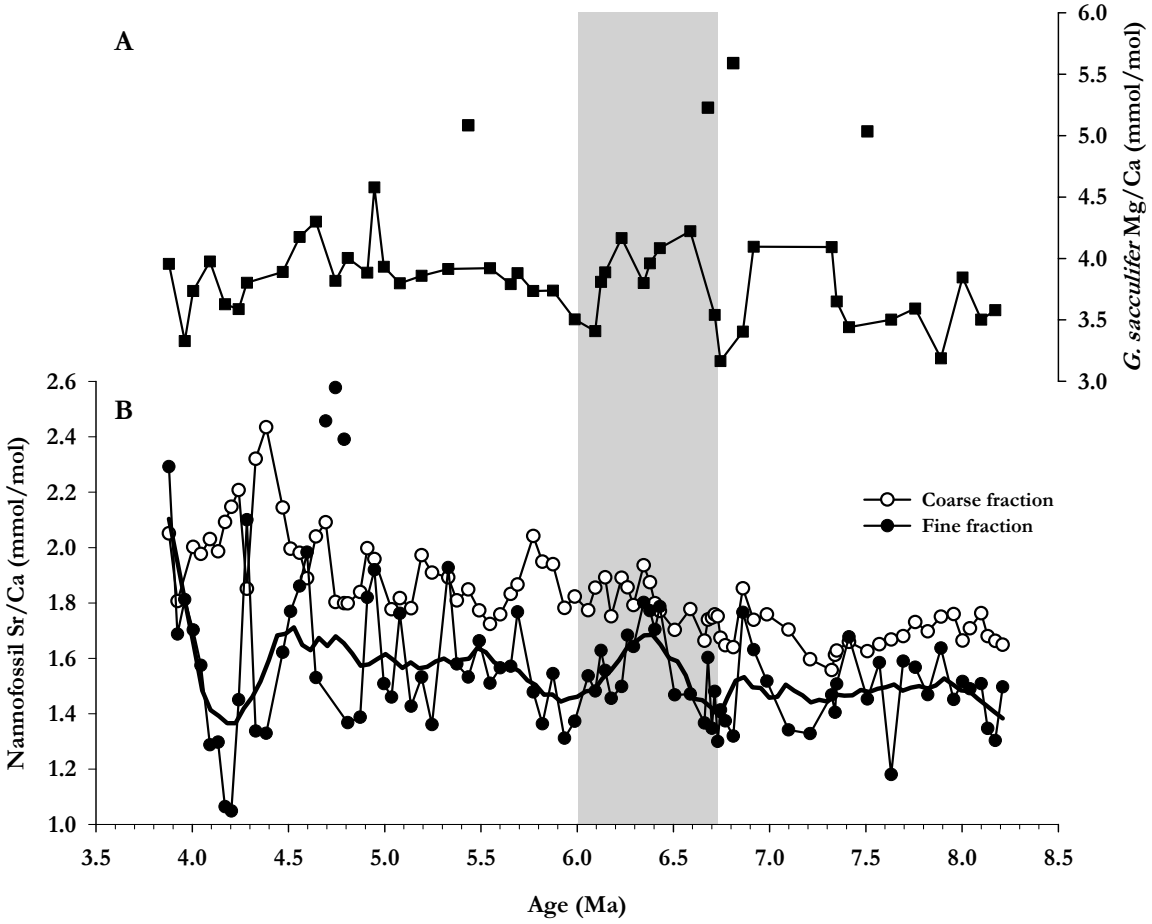

Figure 4.4: ODP Site 925 geochemical records: A) *Globigerinoides sacculifer* Mg/Ca (mmol/mol) and B) coarse and fine fraction nannofossil Sr/Ca (mmol/mol) measured during this project. Singular data points are likely outliers and therefore not used to highlight the long term trend as expressed by the smoothed (10% exponential function) bold line.

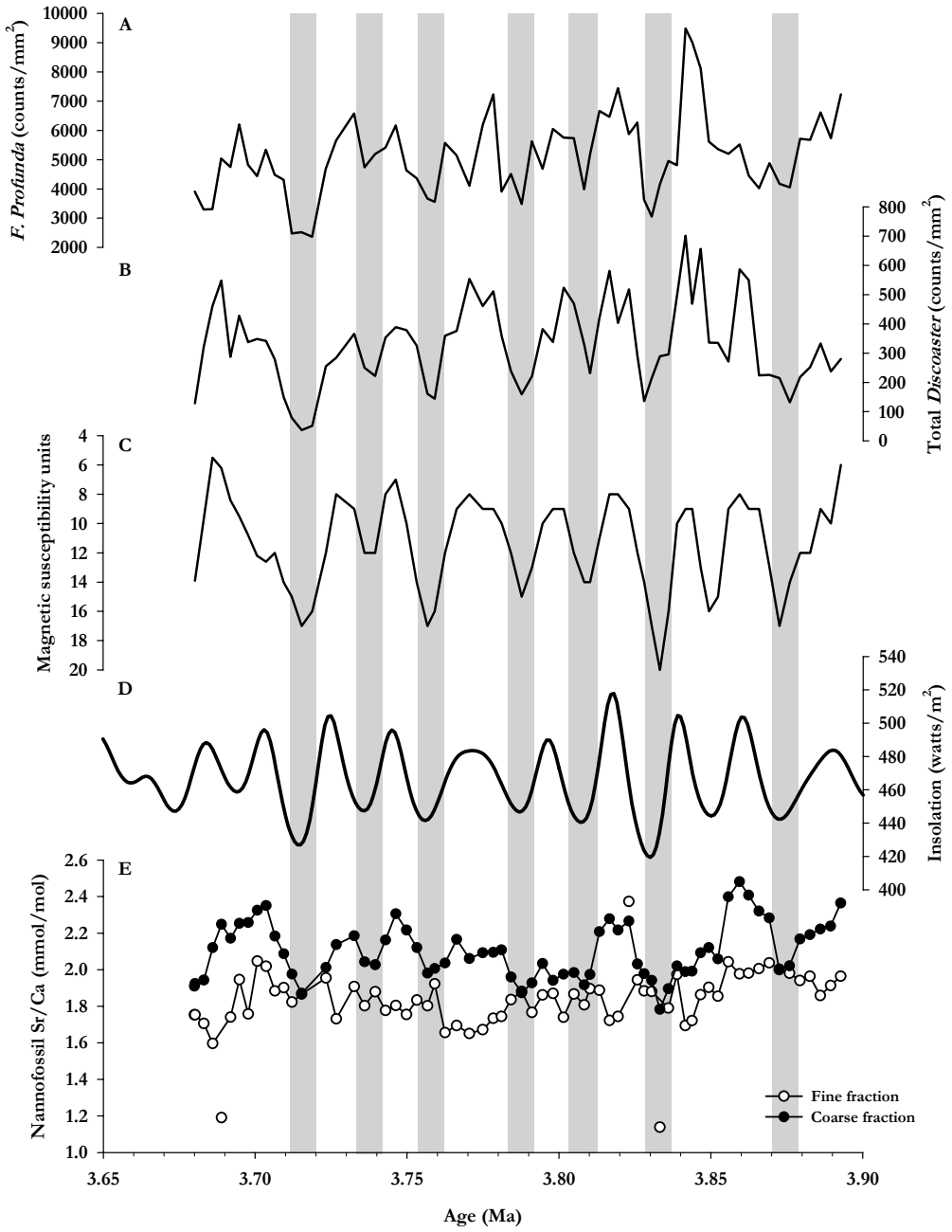

Figure 4.5: ODP Site 926 records: A) *Florisphaera profunda* abundances (counts/mm^2) [Gibbs *et al.*, 2004], B) total *Discoaster* abundances (counts/mm^2) [Gibbs *et al.*, 2004], C) magnetic susceptibility (note inverted axis) [Gibbs *et al.*, 2004], D) curve for insolation (watts/m^2) [Laskar, 1990], and E) coarse and fine fraction nannofossil Sr/Ca (mmol/mol) measured during this project. Singular data points are likely outliers.

APPENDIX A: VIEWING AND IMAGING PROCEDURES

SEM stub production methods

Modified version of methods employed by H. Stoll [pers. comm.]

STEP	PROCEDURE
I	Dilute small amount of sample in 100 µl of weak ammonia solution (~3 ml NH_4OH to 100 ml DIH_2O). If solution is milky, suspend ~30 µl solution in DIH_2O to dilute.
II	Pipette solution into a syringe filtration rig, using .45 µm polycarbonate filters, and filter through.
III	Allow filter to dry completely.
IV	Use a punch to acquire section of the filter for viewing (also, mark section with conductive pen or slip edge for identification in microscope).
IV	Mount filter section to SEM stub with 2-sided carbon stickers.

Smear slide production methods *[S. Gibbs, pers. comm.]*

STEP	PROCEDURE
I	Lick cover slip (saliva helps disaggregate sediment).
II	Scratch small amount of sediment onto cover slip and add one drop of DIH_2O.
III	Use toothpick to disaggregate sediment and smear across cover slip. If clumping occurs or paste is not even, heat on hot plate to remove excess moisture ensuring that smear density varies across the cover slip.
IV	Once satisfied with distribution, dry on hotplate (not too hot).
V	Label glass slide and place two drops of Norland Optical Adhesive on its center.
VI	Place cover slip on the adhesive, sediment side down, and put back on hot plate until adhesive has even dispersed beneath cover slip.
VII	Dry slide on window sill or beneath UV lamp until the adhesive has hardened.

APPENDIX B: ODP SITE 982 DATA

982 Core	Section	Top (cm)	Depth (mcd)	Age (Ma)	Coccolith Sr/Ca_{bulk}
9H	5	53	86.47	3.70	2.01
9H	7	62	89.56	3.77	2.10
10H	1	76	91.47	3.82	2.24
10H	3	32	94.03	3.88	2.04
10H	4	131	96.52	3.94	2.14
10H	6	82	99.03	4.00	2.51
11H	1	43	101.5	4.06	1.96
11H	2	141	104	4.12	1.94
11H	4	91	106.5	4.18	1.85
11H	6	42	109	4.24	1.62
12H	1	51	111.5	4.30	1.95
12H	3	1	114	4.36	1.95
12H	4	101	116.5	4.42	1.90
12H	6	51	119	4.48	1.85
13H	1	1	121.6	4.54	1.92
13H	2	97	124	4.64	1.88
13H	4	41.5	126.5	4.67	1.98
13H	5	146	129	4.72	2.04
13H	CC	16	131.3	4.76	1.92
14H	2	41	134	4.80	2.00
14H	3	140	136.5	4.86	2.22
14H	5	90	139	4.89	1.94
14H	6	90	140.5	4.91	2.20
15H	1	0	143.1	4.94	1.88
15H	2	93	145.5	4.99	2.06
15H	4	43	148	5.03	1.83
15H	5	143	150.5	5.05	1.79
15H	CC	13	152.8	5.08	1.76
16H	2	73	155.5	5.15	1.83
16H	4	123	159	5.22	1.90

982 Core	Section	Top (cm)	Depth (mcd)	Age (Ma)	Coccolith Sr/Ca_{bulk}
16H	7	26	162.5	5.25	1.97
17H	1	141	165	5.28	1.90
17H	2	91	166	5.29	1.90
17H	3	41	167	5.31	1.65
17H	3	141	168	5.35	1.80
17H	4	91	169	5.38	1.90
17H	5	41	170	5.42	1.85
17H	6	91	172	5.48	1.73
18H	1	12	174.2	5.55	1.99
18H	2	42	176	5.60	1.88
18H	3	90	178	5.64	1.91
18H	4	142	180	5.66	1.87
18H	6	42	182	5.72	1.57
18H	CC	10		5.76	1.83
19H	1	121	186	5.81	1.79
19H	3	21	188	5.85	1.88
19H	4	71	190	5.91	1.72
19H	5	121	192	5.95	1.86
19H	7	21	194	5.99	1.79
20H	1	84	196	6.04	1.76
20H	2	134	198	6.08	1.85
20H	4	34	200	6.13	1.84
20H	5	134	202.5	6.17	1.74
20G	CC	10		6.20	1.69
21H	2	41	207.5	6.25	1.76
21H	3	140	210	6.30	1.76
21H	5	22	211.8	6.34	1.80
21H	6	52	213.6	6.38	1.62
22H	1	89	215.4	6.42	1.83
22H	2	120	217.2	6.46	1.80
22H	4	1	219	6.51	1.80
22H	5	31	220.8	6.57	1.84
22H	6	56	222.6	6.63	
23H	1	81	226.4	6.72	1.77
23H	2	108	228.2	6.76	1.76
23H	3	140	230	6.82	1.79
23H	5	21	231.8	6.85	1.81
23H	6	50	233.6	6.88	1.73

982 Core	Section	Top (cm)	Depth (mcd)	Age (Ma)	Coccolith Sr/Ca_{bulk}
24H	2	124	236.7	6.90	1.76
24H	3	4	237	6.94	1.86
24H	4	34	238.8	7.02	1.79
24H	5	64	240.6	7.06	1.73
24H	6	94	242.4	7.11	1.70
25H	1	0	244.6	7.16	1.71
25H	3	21	247.8	7.23	1.78
25H	4	51	249.6	7.27	1.61
25H	5	88	251.5	7.31	1.67
25H	6	110	253.2	7.34	1.65
26H	1	91	255	7.39	1.71
26H	2	121	256.8	7.46	1.88
26H	4	1	258.6	7.53	1.85
26H	5	31	260.4	7.59	1.81
26H	6	63	262.2	7.65	1.82
27X	1	41	264	7.70	1.89
27X	2	69	265.8	7.76	1.84
27X	3	101	267.6	7.81	1.88
27X	4	132	269.4	7.93	1.88
28X	1	132	271.2	8.03	1.74
28X	3	11	273	8.15	1.79
28X	4	41	274.8	8.26	1.72
28X	5	71	276.6	8.40	1.78
29X	1	0	279.5	8.55	1.76
29X	1	0	279.5	8.55	1.76
29X	1	71	280.2	8.60	1.72
29X	2	101	282	8.73	1.74
29X	3	131	283.8	8.85	1.85
29X	4	106	285.1	8.94	1.71

APPENDIX C: ODP SITE 925 DATA

925 Core	Section	Top (cm)	Depth (mcd)	Age (Ma)	Coccolith Sr/Ca_{fine}	Coccolith Sr/Ca_{coarse}
13H	3	93	105.07	3.88	2.29	2.05
13H	4	68	80.07	3.92	1.69	1.81
13H	5	43	55.07	3.96	1.81	
13H	6	18	30.07	4.00	1.70	2.00
13H	6	143	155.07	4.04	1.57	1.98
14H	1	41	53.34	4.09	1.29	2.03
14H	2	16	28.34	4.13	1.30	1.99
14H	2	141	153.34	4.17	1.06	2.09
14H	3	116	128.34	4.20	1.05	2.15
14H	4	91	103.34	4.24	1.45	2.21
14H	5	67	79.34	4.28	2.10	1.85
14H	6	42	54.34	4.33	1.34	2.32
14H	7	16	28.34	4.38	1.33	2.43
15H	1	0	13.31	4.47	1.62	2.14
15H	1	119	132.31	4.51	1.77	2.00
15H	2	94	107.31	4.56	1.86	1.98
15H	3	69	82.31	4.60	1.98	1.89
15H	4	44	57.31	4.64	1.53	2.04
15H	5	19	32.31	4.69	2.46	2.09
15H	5	144	157.31	4.74	2.58	1.80
15H	6	119	132.31	4.79	2.39	1.80
15H	7	24	37.31	4.81	1.37	1.80
16H	1	16	30.82	4.87	1.39	1.84
16H	1	143	157.82	4.91	1.82	2.00
16H	2	118	132.82	4.95	1.92	1.96
16H	3	97	111.82	5.00	1.51	
16H	4	68	82.82	5.04	1.46	1.78
16H	5	43	57.82	5.08	1.76	1.82

925 Core	Section	Top (cm)	Depth (mcd)	Age (Ma)	Coccolith Sr/Ca_{fine}	Coccolith Sr/Ca_{coarse}
16H	6	18	32.82	5.14	1.43	1.78
16H	6	143	157.82	5.19	1.53	1.97
17H	1	8	23.42	5.25	1.36	1.91
17H	1	133	148.42	5.33	1.93	1.89
17H	2	107	122.42	5.38	1.58	1.81
17H	3	83	98.42	5.43	1.53	1.85
17H	4	58	73.42	5.49	1.66	1.77
17H	5	35	50.42	5.55	1.51	1.72
17H	6	8	23.42	5.60	1.57	1.76
17H	6	133	148.42	5.66	1.57	1.83
17H	7	58	73.42	5.69	1.77	1.87
18H	1	38	54.87	5.77	1.48	2.04
18H	2	13	29.87	5.82	1.36	1.95
18H	2	138	154.87	5.87	1.54	1.94
18H	3	114	130.87	5.93	1.31	1.78
18H	4	88	104.87	5.99	1.37	1.82
18H	5	63	79.87	6.06	1.54	1.77
18H	6	38	54.87	6.09	1.48	1.85
18H	7	13	29.87	6.12	1.63	
19H	1	49	66.27	6.15	1.56	1.89
19H	2	23	40.27	6.18	1.46	1.75
19H	2	147	164.27	6.23	1.50	1.89
19H	3	125	142.27	6.26	1.68	1.86
19H	4	97	114.27	6.29	1.64	1.79
19H	5	77	94.27	6.35	1.80	1.94
19H	6	48	65.27	6.38	1.77	1.87
19H	7	23	40.27	6.40	1.70	1.80
20H	1	17	35.08	6.43	1.79	1.77
20H	1	142	160.08	6.51	1.47	1.70
20H	2	117	135.08	6.59	1.47	1.78
20H	3	89	107.08	6.66	1.37	1.66
20H	4	67	85.08	6.68	1.60	1.74
20H	5	40	58.08	6.70	1.35	1.75
20H	6	17	35.08	6.72	1.48	1.76
20H	6	142	160.08	6.73	1.30	1.75

925 Core	Section	Top (cm)	Depth (mcd)	Age (Ma)	Coccolith Sr/Ca_{fine}	Coccolith Sr/Ca_{coarse}
21H	1	121	142.29	6.75	1.41	1.67
21H	2	96	117.29	6.77	1.37	1.65
21H	3	71	92.29	6.81	1.32	1.64
21H	4	46	67.29	6.86	1.77	1.85
21H	5	21	42.29	6.92	1.63	1.74
21H	5	146	167.29	6.99	1.52	1.76
21H	6	121	142.29	7.10	1.34	1.70
22H	1	4	25.71	7.21	1.33	1.60
22H	1	129	150.71	7.32	1.47	1.56
22H	2	115	136.71	7.34	1.40	1.61
22H	3	70	91.71	7.35	1.51	1.63
22H	4	51	72.71	7.41	1.68	1.66
22H	5	29	50.71	7.51	1.45	1.63
22H	6	4	25.71	7.57	1.58	1.65
22H	6	127	148.71	7.63	1.18	1.67
22H	7	67	88.71	7.69	1.59	1.68
23H	1	24	48.51	7.76	1.57	1.73
23H	1	148	172.51	7.82	1.47	1.70
23H	2	124	148.51	7.89	1.64	1.75
23H	3	99	123.51	7.96	1.45	1.76
23H	4	74	98.51	8.00	1.52	1.66
23H	5	49	73.51	8.04	1.49	1.71
23H	6	24	48.51	8.10	1.51	1.76
23H	6	148	172.51	8.13	1.35	1.68
24H	1	8	33.17	8.17	1.30	1.66
24H	1	133	158.17	8.21	1.50	1.65

ODP Site 925 *Globigerinoides sacculifer* chemistry

925 Core	Sec	Top (cm)	Depth (mcd)	Age Ma	*G. sacculifer* Sr/Ca	*G. sacculifer* Mg/Ca	*G. sacculifer* Mn/Ca
13H	3	93	105.07	3.88	1.36	3.96	0.27
13H	4	68	80.07	3.92			
13H	5	43	55.07	3.96	1.40	3.33	0.23
13H	6	18	30.07	4.00	1.36	3.73	0.28
13H	6	143	155.07	4.04			
14H	1	41	53.34	4.09	1.26	3.98	0.24
14H	2	16	28.34	4.13			
14H	2	141	153.34	4.17	1.26	3.63	0.27
14H	3	116	128.34	4.20			
14H	4	91	103.34	4.24	1.27	3.59	0.25
14H	5	67	79.34	4.28	1.27	3.80	0.27
14H	6	42	54.34	4.33			
14H	7	16	28.34	4.38			
15H	1	0	13.31	4.47	1.22	3.89	0.23
15H	1	119	132.31	4.51			
15H	2	94	107.31	4.56	1.24	4.18	0.21
15H	3	69	82.31	4.60			
15H	4	44	57.31	4.64	1.28	4.30	0.22
15H	5	19	32.31	4.69			
15H	5	144	157.31	4.74	1.22	3.82	0.20
15H	6	119	132.31	4.79			
15H	7	24	37.31	4.81	1.24	4.00	0.17
16H	1	16	30.82	4.87			
16H	1	143	157.82	4.91	1.25	3.88	0.22
16H	2	118	132.82	4.95	1.28	4.58	0.24
16H	3	97	111.82	5.00	1.23	3.93	0.23
16H	4	68	82.82	5.04			
16H	5	43	57.82	5.08	1.21	3.80	0.25
16H	6	18	32.82	5.14			
16H	6	143	157.82	5.19	1.27	3.86	0.26
17H	1	8	23.42	5.25			
17H	1	133	148.42	5.33	1.22	3.91	0.22
17H	2	107	122.42	5.38			

925 Core	Sec	Top (cm)	Depth (mcd)	Age Ma	*G. sacculifer* Sr/Ca	*G. sacculifer* Mg/Ca	*G. sacculifer* Mn/Ca
17H	3	83	98.42	5.43	1.23	5.08	0.27
17H	4	58	73.42	5.49			
17H	5	35	50.42	5.55	1.15	3.92	0.26
17H	6	8	23.42	5.60			
17H	6	133	148.42	5.66	1.14	3.79	0.26
17H	7	58	73.42	5.69	1.17	3.88	0.30
18H	1	38	54.87	5.77	1.19	3.73	0.22
18H	2	13	29.87	5.82			
18H	2	138	154.87	5.87	1.16	3.74	0.26
18H	3	114	130.87	5.93			
18H	4	88	104.87	5.99	1.18	3.50	0.22
18H	5	63	79.87	6.06			
18H	6	38	54.87	6.09	1.15	3.41	0.27
18H	7	13	29.87	6.12	1.20	3.81	0.32
19H	1	49	66.27	6.15	1.13	3.89	0.27
19H	2	23	40.27	6.18			
19H	2	147	164.27	6.23	1.17	4.17	0.37
19H	3	125	142.27	6.26			
19H	4	97	114.27	6.29			
19H	5	77	94.27	6.35	1.21	3.80	0.28
19H	6	48	65.27	6.38	1.15	3.96	0.44
19H	7	23	40.27	6.40			
20H	1	17	35.08	6.43	1.15	4.08	0.34
20H	1	142	160.08	6.51			
20H	2	117	135.08	6.59	1.19	4.22	0.24
20H	3	89	107.08	6.66			
20H	4	67	85.08	6.68	1.18	5.23	0.40
20H	5	40	58.08	6.70			
20H	6	17	35.08	6.72	1.10	3.54	0.37
20H	6	142	160.08	6.73			
21H	1	121	142.29	6.75	1.20	3.16	0.20
21H	2	96	117.29	6.77			
21H	3	71	92.29	6.81	1.17	5.59	0.32
21H	4	46	67.29	6.86	1.14	3.40	0.24
21H	5	21	42.29	6.92	1.18	4.10	0.43

925 Core	Sec	Top (cm)	Depth (mcd)	Age Ma	*G. sacculifer* Sr/Ca	*G. sacculifer* Mg/Ca	*G. sacculifer* Mn/Ca
21H	5	146	167.29	6.99			
21H	6	121	142.29	7.10			
22H	1	4	25.71	7.21			
22H	1	129	150.71	7.32	1.15	4.09	0.44
22H	2	115	136.71	7.34			
22H	3	70	91.71	7.35	1.18	3.65	0.33
22H	4	51	72.71	7.41	1.17	3.44	0.25
22H	5	29	50.71	7.51	1.18	5.03	0.31
22H	6	4	25.71	7.57			
22H	6	127	148.71	7.63	1.13	3.50	0.22
22H	7	67	88.71	7.69			
23H	1	24	48.51	7.76	1.13	3.59	0.24
23H	1	148	172.51	7.82			
23H	2	124	148.51	7.89	1.14	3.19	0.17
23H	3	99	123.51	7.96			
23H	4	74	98.51	8.00	1.11	3.85	0.19
23H	5	49	73.51	8.04			
23H	6	24	48.51	8.10	1.27	3.50	0.19
23H	6	148	172.51	8.13			
24H	1	8	33.17	8.17	1.20	3.58	0.21
24H	1	133	158.17	8.21			

APPENDIX D: ODP SITE 926 DATA

926 Core	Section	Top (cm)	Age (Ma)	Depth (mcd)	Nannofossil Sr/Ca_{fine}	Nannofossil Sr/Ca_{coarse}
12H	2	125	3.680		1.75	1.91
12H	2	135	3.680	114.22	1.75	1.92
12H	2	145	3.683	114.32	1.71	1.94
12H	3	5	3.686	114.42	1.60	2.12
12H	3	15	3.689	114.52	1.19	2.25
12H	3	25	3.692	114.62	1.74	2.17
12H	3	35	3.695	114.72	1.95	2.25
12H	3	45	3.698	114.82	1.76	2.26
12H	3	55	3.701	114.92	2.05	2.32
12H	3	65	3.704	115.02	2.02	2.35
12H	3	75	3.707	115.12	1.88	2.18
12H	3	85	3.709	115.22	1.90	2.09
12H	3	94	3.712	115.32	1.82	1.98
12H	3	105	3.715	115.42	1.87	1.87
12H	3	115	3.719	115.52		
12H	3	128	3.723	115.62	1.95	2.01
12H	3	138	3.727	115.72	1.73	2.14
12H	4	5	3.733	115.92	1.91	2.19
12H	4	15	3.736	116.02	1.80	2.04
12H	4	25	3.740	116.12	1.88	2.03
12H	4	35	3.743	116.22	1.78	2.16
12H	4	45	3.746	116.32	1.80	2.31
12H	4	55	3.750	116.42	1.75	2.22
12H	4	65	3.753	116.52	1.83	2.12
12H	4	75	3.757	116.62	1.80	1.98
12H	4	82	3.759	116.69	1.92	2.01
12H	4	92	3.763	116.79	1.66	2.04
12H	4	103	3.766	116.90	1.69	2.17
12H	4	115	3.771	117.02	1.65	2.06

926 Core	Section	Top (cm)	Age (Ma)	Depth (mcd)	Nannofossil Sr/Ca_{fine}	Nannofossil Sr/Ca_{coarse}
12H	4	128	3.775	117.15	1.67	2.09
12H	4	138	3.778	117.25	1.73	2.10
12H	4	146	3.781	117.33	1.74	2.11
12H	5	5	3.784	117.42	1.84	1.96
12H	5	15	3.788	117.52	1.88	1.87
12H	5	25	3.791	117.62	1.77	1.93
12H	5	35	3.795	117.72	1.86	2.03
12H	5	45	3.798	117.82	1.87	1.94
12H	5	55	3.802	117.92	1.74	1.97
12H	5	65	3.805	118.02	1.87	1.98
12H	5	75	3.808	118.12	1.81	1.92
12H	5	82	3.810	118.22	1.90	1.97
12H	5	93	3.813	118.32	1.89	2.21
12H	5	105	3.817	118.42	1.72	2.28
12H	5	115	3.819	118.52	1.74	2.22
12H	5	128	3.823	118.62	2.37	2.27
12H	5	138	3.826	118.72	1.94	2.03
12H	5	146	3.828	118.82	1.88	1.98
12H	6	5	3.831	118.92	1.88	1.94
12H	6	15	3.833	119.02	1.14	1.78
12H	6	25	3.836	119.12	1.79	1.90
12H	6	35	3.839	119.22	1.97	2.02
12H	6	45	3.842	119.32	1.69	1.99
12H	2	27	3.844	119.89	1.72	1.99
12H	2	37	3.847	119.49	1.86	2.09
12H	2	47	3.849	119.59	1.90	2.12
12H	2	57	3.852	119.69	1.85	2.06
12H	2	67	3.856	119.79	2.04	2.40
12H	2	77	3.859	119.90	1.98	2.48
12H	2	87	3.862	119.99	1.98	2.41
12H	2	97	3.866	120.09	2.01	2.32
12H	2	107	3.869	120.19	2.04	2.28
12H	2	117	3.873	120.29	2.00	2.00
12H	2	127	3.876	120.39	1.98	2.02
12H	2	137	3.879	120.49	1.94	2.17

926 Core	Section	Top (cm)	Age (Ma)	Depth (mcd)	Nannofossil Sr/Ca_{fine}	Nannofossil Sr/Ca_{coarse}
12H	2	147	3.883	120.59	1.96	2.19
12H	3	7	3.886	120.69	1.86	2.22
12H	3	17	3.889	120.79	1.91	2.24
12H	3	27	3.893	120.89	1.96	2.36

REFERENCES

Andersson, C., Jansen, E., 2003. A Miocene (8-12 Ma) intermediate water benthic stable isotope record from the northeastern Atlantic, ODP Site 982. *Paleoceanography* 18(1), 1013, doi: 10.1029/2001PA000657.

Antoine, D., Andre, J.M., Morel, A., 1996. Oceanic primary production 2. Estimation at global scale from satellite (coastal zone color scanner) chlorophyll. *Global Biogeochemical Cycles* 10, 57-69.

Apitz, S.E., 1991. The lithification of ridge flank basal carbonates: Characterization and implications for Sr/Ca and Mg/Ca in marine chalks and limestones. PhD dissertation, University of California, San Diego, CA.

Backman, J., Pestiaux, P., 1987. Pliocene *Discoaster* abundance variations, Deep Sea Drilling Project Site 606; biochronology and paleoenvironmental implications. In: Ruddiman, W.F., Kidd R.B., *et al.* (Eds.) *Initial Reports Deep Sea Drilling Project* 94, pp. 903-910.

Backman, J., Pestiaux, P., Zimmerman, H., Hermelin, O., 1986. Paleoclimatic and paleoceanographic development in the Pliocene North Atlantic; *Discoaster* accumulation and coarse fraction data. *Special Papers, Geologic Society of London* 21, 231-242.

Bairbakesh, A.N., Jollman, J., Sprengel, C., Thierstein, H.R., 1999. Disintegration of aggregates and coccospheres in sediment trap samples. *Marine Micropaleontology* 37, 219-223.

Bassinot, F.C., Beaufort, L., Vincent, E., Labeyrie, L., 1997. Changes in dynamics of western equatorial Atlantic surface currents and biogenic productivity at the "Mid-Pleistocene revolution" (~930 ka). In: Shackleton, N.J., Curry, *et al.* (Eds.), *Proceedings of the Ocean Drilling Program Scientific Results* 154, pp. 269-284.

Beaufort, l., Lancelot., Y., Camberlin, P., Cayre, O., Vincent, E., Bassinot, F., Labeyrie, L., 1997. Insolation cycles as a major control of equatorial Indian Ocean primary production. *Science* 278, 1451-1454.

Berger, W.H., Leckie, R.M., Janecek, T.R., Stax, R., Takayama, T., 1993. Neogene carbonate sedimentation on Ontong Java Plateau: highlights and open questions. In: Berger, W.H., Kroenke, L.W., *et al.* (Eds.), *Proceedings of the Ocean Drilling Program Scientific Results* 130, pp. 711-744.

Berger, W.H., Wefer, G., 1990. Export production: seasonality and intermittency, and paleoceanographic implications. *Paleogeography, Paleoclimatology, Paleoecology* 89, 245-254.

Billups, K., Rickaby, R., Schrag, D.P., 2004. Cenozoic pelagic Sr/Ca records: Exploring a link to paleoproductivity, *Paleoceanography,* 19, 3005, doi: 10.1029/2004PA001011.

Bown, P.R. (Ed.), 1998. Calcareous nannofossil biostratigraphy. Chapman & Hall (Kluwer Academic Publishing), London, UK, 283 pp.

Boyd, P.W., Newton, P.P., 1999. Does planktonic community structure determine downward particulate organic carbon flux in different oceanic provinces? *Deep-Sea Research* 46, 63-91.

Bralower, T.J., 2002. Evidence of surface water oligotrophy during the Paleocene-Eocene thermal maximum: Nannofossil assemblage data from Ocean Drilling Program Site 690, Maud Rise, Weddell Sea. *Paleoceanography* 17(2), 1023, doi: 10.1029/2001PA000662.

Broecker, W. S., Peng, T.H., 1982. Tracers in the Sea. Lamont-Doherty Geological Observatory, Columbia University, Palisades, NY, pp. 25-28.

Brown, S.J., Elderfield, H., 1996. Variations in Mg/Ca and Sr/Ca ratios in planktonic foraminifera caused by post-depositional dissolution: Evidence for shallow Mg-dependent dissolution. *Paleoceanography* 11(5), 543-551.

Brownlee, C., Taylor, A., 2004. Calcification in coccolithophores: A cellular perspective, In: Thierstein, H.R., Young, J.R. (Eds.), *Coccolithophores- from molecular processes to global impact*. Springer-Verlag, Berlin, pp. 31-50.

Carpenter, S.J., Lohmann, K.C., 1992. Sr/Mg ratios of modern marine calcite: Empirical indicators of ocean chemistry and precipitation rates. *Geochimica Cosmochimica Acta* 56, 1837-1849.

Chapman, M.R., Chepstow-Lusty, A.J., 1997. Late Pliocene climatic changes and the global extinction of the *discoasters*: an independent assessment using oxygen isotope record. *Palaeogeography, Palaeoclimatology, Palaeoecology* 134, 109–125.

Chepstow-Lusty, A., Backman, J., Shackleton, N.J., 1989. Comparison of Upper Pliocene *Discoaster* abundance variations from North Atlantic Sites 552, 607, 658, 659, and 662: further evidence for marine plankton responding to orbital forcing. In: Ruddiman, W., Sarnthein, M., *et al.* (Eds.), *Proceedings of the Ocean Drilling Program Scientific Results* 108, pp. 121-140.

Chepstow-Lusty, A., Backman, J., Shackleton, N.J., 1991. Paleoclimatic control of upper Pliocene *Discoaster* assemblages in the North Atlantic. *Journal of Micropaleontology* 9(2), 133-143.

Cortés, M.Y., Bollmann, J., Thierstein, H.R., 2001. Coccolithophore ecology at the HOT station ALOHA, Hawaii. *Deep-Sea Research Part II* 48(8-9), 1957-1981.

Curry, W.B., Shackleton, N.J., Richter, C., Bralower, T.J., 1995. Site 925 and Site 926. *Proceedings of the Ocean Drilling Program Initial Reports* 154, College Station, TX (ODP), pp. 55-232.

Delaney, M.L., Filippelli, G.M., 1994. An apparent contradiction in the role of phosphorous in Cenozoic chemical mass balances for the world ocean. *Paleoceanography* 9(4), 13-527.

Dickens, G.R., Owen, R.M., 1999. The latest Miocene-Early Pliocene biogenic bloom: a revised Indian Ocean perspective. *Marine Geology* 161, 75-91.

Diester-Haass, L., Billups, K., Emeis, K.C., in press. In search of the late Miocene–early Pliocene 'biogenic bloom' in the Atlantic Ocean (ODP Sites 982, 925, and 1088). *Paleoceanography*.

Diester-Haass, L., Meyers, P.A., Bickert, T., 2004. Carbonate crash and biogenic bloom in the late Miocene: Evidence from ODP Sites 1085, 1086 and 1087 in the Cape Basin, southeast Atlantic Ocean. *Paleoceanography* 19(1), PA1007 doi: 10.1029/2003PA000933.

Diester-Haass, L., Nees, S., 2004. Late Neogene history of paleoproductivity and ice rafting South of Tasmania. In: Exon, N.F., Kennett, J.P., Malone, M.J. (Eds.), *The Cenozoic Southern Ocean: Tectonics, Sedimentation, and Climate Change Between Australia and Antarctica, Geophysical Monograph Series* 148, American Geophysical Union, doi: 10.1029/148GM18.

Farrell, J.W., Raffi, I., Janecek, T.R., Murray, D.W., Levitan, M., Dadey, K.A., Emeis, K.C., Lyle, M., Flores, J.A., Hovan, S., 1995. Late Neogene sedimentation patterns in the eastern equatorial Pacific. In: Pisias, N.G., Mayer, *et al.* (Eds.), *Proceedings of the Ocean Drilling Program Scientific Results* 138, pp. 717-756.

Filippelli, G.M., 1997. Intensification of the Asian monsoon and a chemical weathering event in the late Miocene-early Pliocene: Implications for late Neogene climate change. *Geology* 25, 27-30.

Flores, J.A., Sierro, F.J., Raffi, I., 1995. Evolution of the calcareous nannofossil assemblage as a response to the paleoceanographic changes in the eastern equatorial Pacific Ocean. In: Pisias, N.G., Mayer, *et al.* (Eds.), *Proceedings of the Ocean Drilling Program Scientific Results* 138, pp. 163-176.

Flores, J.A., Sierro, F.J., Filippelli, G.M., Bárcena, M.A., Pérez-Folgado, M., Vázquez, A., Utrilla, R., 2005. Surface water dynamics and phytoplankton communities during the deposition of cyclic late Messinian sapropel sequences in the western Mediterranean. *Marine Micropaleontology* 56, 50-79.

Francois, R., Honjo, S., Krishfield, R., Manganini, S., 2002. Factors controlling the flux of organic carbon to the bathypelagic zone in the ocean. *Global Biogeochemical Cycles* 16(4), 1087, doi: 10.1029/2001GB001722.

Gibb, S., Shackleton, N., Young, J., 2004. Orbitally forced climate signals in mid-Pliocene nannofossil assemblages. *Marine Micropaleontology* 51, 39-56.

Grant, K.M., Dickens, G.R., 2002. Coupled productivity and carbon isotope records in the southwest Pacific Ocean during the late Miocene-early Pliocene biogenic bloom. *Paleogeography, Paleoclimatology, Paleoecology* 187, 61-82.

Gupta, A.K., Thomas, E., 1999. Latest Miocene-Pleistocene productivity and deep-sea ventilation in the northwestern Indian Ocean (Deep Sea Drilling Project site 219). *Paleoceanography* 14, 62-73.

Haidar, A.T., Thierstein, H.R., 2001. Coccolithophore dynamics off Bermuda (N. Atlantic). *Deep-Sea Research Part II* 48, 1925-1956.

Hampt-Andreasen, G., Delaney, M.L., 2000. Bulk calcite size fraction distribution and Sr/Ca composition for deep-sea sediments at selected age horizons. *Marine Geology* 169, 185-205.

Haq, B.U., Lohmann, G.P., 1976. Early Cenozoic calcareous nannoplankton biogeography of the Atlantic Ocean. *Marine Micropaleontology* 1, 119-194.

Herguera, J.C., Berger, W.H., 1991. Paleoproductivity from benthic foraminifera abundance: glacial to postglacial changes in the west-equatorial Pacific. *Geology* 19, 1173-1176.

Hermoyian, C.S., Owen, R.M., 2001. Late Miocene-early Pliocene biogenic bloom: evidence from low productivity regions of the Indian and Atlantic Oceans. *Paleoceanography* 16(1), 95–100.

Herguera, J.C., 2000. Last glacial paleoproductivity patterns in the eastern equatorial Pacific: benthic foraminifera records. *Marine Micropaleontology* 40, 259-275.

Hodell, D.A., Curtis, J.H., Sierro, F.J., Raymo, M.E., 2001. Correlation of late Miocene to early Pliocene sequences between the Mediterranean and North Atlantic. *Paleoceanography* 16(2), 164-178.

Jansen, E., Raymo, M.E., Blum, P., *et al.*, 1996. Site 982. *Proceedings of the Ocean Drilling Program Initial Reports* 162, College Station, TX (ODP), pp. 91-138.

Lampitt, R.S., Antia, A.N., 1997. Particle flux in deep seas: Regional characteristics and temporal variability. *Deep-Sea Research* 44(8), 1377-1403.

Laskar, J., 1990. The chaotic motion of the solar system: a numerical estimate of the size of the chaotic zones. *Icarus* 88, 266-291.

Lear, C.H., Elderfield, H., Wilson, P.A., 2000. Cenozoic deep-sea temperatures and global ice volumes from Mg/Ca in benthic foraminiferal calcite. *Science* 278, 269-272.

Lear, C.H., Elderfield, H., Wilson, P.A., 2003. A Cenozoic seawater Sr/Ca record from benthic foraminiferal calcite and its application in determining global weathering fluxes. *Earth and Planetary Science Letters* 208, 69-84.

Levitus, S., Boyer, T., 1994. World Ocean Atlas 1994 Volume 4: Temperature. National Oceanographic and Atmospheric Administration Atlas NESDIS 4, U.S. Department of Commerce, Washington, D.C..

Lohmann, G.P., Carlson, J.J., 1981. Oceanographic significance of Pacific late Miocene calcareous nannoplankton. *Marine Micropaleontology* 6, 553-579.

Lorens, R.B., 1981. Sr, Cd, Mn and Co distribution coefficients in calcite as a function of precipitation rate. *Geochimica et Cosmochimica Acta* 45, 553-561.

Lyle, M., Dadey, K.A., Farrell, J.W., 1995. The late Miocene (11-8 Ma) eastern Pacific carbonate crash: evidence for reorganization of deep-water circulation by the closure of the Panama gateway. In: Pisias, N.G., Mayer, *et al.* (Eds.), *Proceedings of the Ocean Drilling Program Scientific Results* 138, pp. 821-838.

McCartney, M.S., 1992. Recirculating components to the deep boundary current of the northern North-Atlantic. *Progressive Oceanography* 29(4), 283-383.

McIntyre, A., Molfino, B., 1996. Forcing of Atlantic equatorial and subpolar millennial cycles by precession. *Science* 274, 1867-1869.

Mix, A.C., Pisias, N.G., Rugh, W., Wilson, J., Morey, A., Hagleberg, T.K., 1995. Benthic foraminifera stable isotope record from Site 849, 0-5 Ma: local and global climate changes. In: Pisias, N.G., Mayer, *et al.* (Eds.), *Proceedings of the Ocean Drilling Program, Scientific Results* 138, pp. 371-412.

Molfino, B., McIntyre, A., 1990: A. Precessional forcing of nutricline dynamics in the Equatorial Atlantic. *Science* 249, 766-769.

Murray, D.W., Peterson, L.C., 1997. Biogenic carbonate production and preservation changes between 5 and 10 Ma from the Ceara Rise, western equatorial Atlantic. In: Shackleton, N.J., Curry, *et al.* (Eds.), *Proceedings of the Ocean Drilling Program Scientific Results* 154, pp. 375-388.

Nees, S., 1997. Late Quaternary Paleoceanography of the Tasman Sea: the benthic foraminiferal view. *Paleogeography, Paleoclimatology, Paleoecology* 131, 365-389.

Niemitz, M.D., Billups, K., 2005. Millennial-scale variability in western tropical Atlantic surface ocean hydrography during the early Pliocene. *Marine Micropaleontology* 54, 155-166.

Okada, H., Honjo, S., 1973. The distribution of oceanic coccolithophorids in the Pacific. *Deep-Sea Research Part I* 20, 355-374.

Parker, L.F., Berger, W.H., 1971. Faunal and solution patterns of planktonic foraminifera in surface sediments of the South Pacific. *Deep-Sea Research* 18, 73-107.

Peterson, L.C., Murray, D.W., Ehrmann, W.U., Hempel, P., 1992. Cenozoic carbonate accumulation and compensation depth changes in the Indian Ocean. In: Duncan, R.A., Rea, D.K., *et al.* (eds.), *The Indian Ocean: A synthesis of Results from the Ocean Drilling Program, Geophysical Monograph* 70, American Geophysical Union, pp. 311-333.

Rea, D.K., Basov, I.A., Krissek, L.A., Leg 145 Scientific Party, 1995. Scientific results of drilling in the North Pacific transect. In: Rea, D.K., Basov, I.A., *et al.* (Eds.), *Proceedings of the Ocean Drilling Program, Scientific Results* 145, pp. 577-596.

Richter, F.M., Liang, Y., 1993. The rate and consequences of Sr diagenesis in deep-sea carbonates. *Earth and Planetary Science Letters* 117, 553-565.

Rickaby, R.E.M., Schrag, D.P., Zondervan, I., Riebesell, U., 2002. Growth-rate dependence of Sr incorporation during calcification of *Emiliania huxleyi*. *Global Biogeochemical Cycles* 16(1), doi: 10.1029/20001GB001408.

Rosenthal, Y., Perron-Cashman, S., *et al.*, 2004. Laboratory inter-comparison study of Mg/Ca and Sr/Ca measurements in planktonic foraminifera for paleoceanographic research. *Geochemistry, Geophysics, Geosystems*, doi: 10.1029/2003GC000650.

Rost, B., Riebesell, U., 2004. Coccolithophores and the biological pump: responses to environmental changes. In: Thierstein, H.R., Young, J.R. (Eds.), *Coccolithophores-From Molecular Processes to Global Impact*. Springer-Verlag, Berlin, pp. 76-99.

Scheiderich, K.D., 2004. Paired Mg/Ca and oxygen isotopes of Neogene foraminifera: Pacific and Indian Ocean tropic-subtropic Paleoceanography and paleoclimate. MS thesis, University of Delaware, Newark, DE, 143 pp.

Schmiedl, G., Mackensen, A., 1997. Late quaternary paleoproductivity and deep water circulation in the eastern South Atlantic Ocean: evidence from benthic foraminifera. *Paleogeography, Paleoclimatology, Paleoecology* 130, 43-80.

Schmitz, W.J., McCartney, M.S., 1993. On the North Atlantic circulation. *Reviews of Geophysics* 31, 29-50.

Schrag, D.P., 1999. Rapid analysis of high precision Sr/Ca ratios in corals and other marine carbonates. *Paleoceanography* 14, 97-102.

Shackleton, N.J., Crowhurst, S., 1997. Sediment Fluxes based on an orbitally tuned time scale 5 Ma to 14 Ma, Site 926. In: Shackleton, N.J., Curry, *et al.* (Eds.), *Proceedings of the Ocean Drilling Program Scientific Results* 154, pp. 69-82.

Stoll, H.M., 2005. Limited range of interspecific vital effects in coccolith stable isotopic records during the Paleocene-Eocene thermal maximum. *Paleoceanography* 20, doi: 10.1029/2004PA001046.

Stoll, H.M., Bains, S., 2003. Coccolith Sr/Ca records of productivity during the Paleocene-Eocene thermal maximum from the Weddell Sea. *Paleoceanography* 18(2), 1049, doi: 10.1029/2002PA000875.

Stoll, H.M., Klaas, C., Probert, I., Encinar, J.R., Alonso, J.I.G., 2002a. Calcification rate and temperature effects on Sr partitioning in coccoliths of multiple species of coccolithophorids in culture. *Global and Planetary Change* 34, 153–171.

Stoll, H.M., Rosenthal, Y., Falkowski, P., 2002b. Climate proxies from Sr/Ca of coccolith calcite: Calibrations from continuous culture of *Emiliania Huxleyi*. *Geochimica et Cosmochimica Acta* 66, 927–936.

Stoll, H.M., Schrag, D.P., 2000. Coccolith Sr/Ca as a new indicator of coccolithophorid calcification and growth rate, *Geochemistry, Geophysics, Geosystems* 1(5), doi: 10.1029/1999GC000015.

Stoll, H.M., Schrag, D.P., 2001. Sr/Ca variations in Cretaceous carbonates: relation to productivity and sea level changes. *Paleogeography, Paleoclimatology, Paleoecology* 168, 311–336.

Stoll, H.M., Ziveri, P., 2002. Separation of monospecific and restricted coccolith assemblages from sediments using differential settling velocity. *Marine Micropaleontology* 46, 209-221.

Stoll, H.M., Ziveri, P., 2004. Coccolithophorid-based geochemical paleoproxies. In: Thierstein, H.R., Young, J.R. (Eds.), *Coccolithophores- From Molecular Processes to Global Impact*. Springer-Verlag, Berlin, pp. 528-552.

Stoll, H.M., Ziveri, P., Geisen, M., Probert, I., Young, J.R., 2002c. Potential and limitations of Sr/Ca ratios in coccolith carbonate: new perspectives from cultures and monospecific samples from sediments, *Philosophical Transactions of the Royal Society of London* A360, 719–747.

Stout, P.M., 1985. Interstitial water chemistry and diagenesis of biogenic sediments from the eastern equatorial Pacific, Deep Sea Drilling Project Leg 85. In: Mayer, L., Theyer, F., *et al.* (Eds.)*, Initial Reports Deep Sea Drilling Project* 85*, pp.* 805-820.

Summerhayes, C.P., Emeis, K.C., Angel, M.V., Smith, R.L., Zeitschel, B., 1995. Upwelling in the ocean: modern processes and ancient records, *Reports of the Dahlem Workshop*, John Wiley & Sons, New York, 422 pp.

Tiedemann, R., Franz, S.O., 1997. Deep water circulation, chemistry, and terrigenous sediment supply in the equatorial Atlantic during the Pliocene, 3.3-2.6 Ma and 5-4.5 Ma. In: Shackleton, N.J., Curry, *et al.* (Eds.), *Proceedings of the Ocean Drilling Program, Scientific Results* 154, pp. 299-318.

Van der Zwaan, G.J., Duijnstee, I.A.P., den Bulk, M., Jannink, N.T., Kouwenhoven, T.J., 1999. Benthic foraminifers: proxies or problems? A review of paleoecological concepts. *Earth Science Reviews* 46, 213-236.

Watson, E.B., 1996. Surface enrichment and trace-element uptake during crystal growth. *Geochimica et Cosmochimica Acta* 60, 5013-5020.

Watson, E.B., 2004. A conceptual model for near-surface kinetic controls on the trace-element and stable isotope composition of abiogenic calcite crystals. *Geochimica et Cosmochimica Acta* 68(7) 1473-1488.

Westbroek P., Brown, C.W., Van Bleijswijk, J., Brownlee, C., Brummer, G.J., Conte, M., Egge, J., Fernández, E., Jordan, R., Knappertsbusch, M., Stefels, J., Veldhuis, M., Van der Wal, P., Young, J., 1993. A model system approach to biological climate forcing: the example of *Emiliania huxleyi. Global and Planetary Change* 8, 27-46.

Westbroek, P., Buddemeier, B., Coleman, M., Kok, D.J., Fautin, D., Stal, L., 1994. Strategies for the study of climate forcing by calcification. *Bulletin de l'Institute oceanographique, Monaco* 13, 37-60.

Winter, A., Siesser, W.G. (Eds.), 1994. Coccolithophores. Cambridge University Press, Cambridge, UK, 252 pp.

Yamanaka, Y., Tajika, E., 1996. The role of the vertical fluxes of particulate organic matter and calcite in the oceanic carbon cycle: Studies using an ocean biogeochemical general circulation model. *Global Biogeochemical Cycles* 10(2), 361-382.

Yasuda, H., 1997. Late Miocene-Holocene Paleoceanography of the western equatorial Atlantic: evidence from deep-sea benthic foraminifera. In: Shackleton, N.J., Curry, *et al.* (Eds.), *Proceedings of the Ocean Drilling Program, Scientific Results* 154, pp. 395-432.

Ziveri, P., Thunell, R., Rio, D., 1995. Export production of coccolithophores in an upwelling region: Results from San Pedro Basin, Southern California Bight. *Marine Micropaleontology* 24, 335-358.